CHAPTER IV
RESULTS AND DISCUSSION

The discussion of the results in this experiment will be provided in six main topics and each topic will be discussed by relating to the observation from previous works.

1. Characterization of Polymer Properties
2. Processing and Rheological Characteristics
3. Morphology of the Blends
4. Molecular Orientation
5. Thermal Properties
6. Mechanical Properties of Blend Films

4.1 Characterization of polymer properties

4.1.1 Weight Average Molecular Weight (M_w), Number Average Molecular Weight (M_n) and Molecular Weight Distribution (MWD)

4.1.1.1 Linear Low Density Polyethylene (LLDPE)

Table 4.1 Characteristics of LLDPE.

Characteristics	Value
Density (g/cm^3)	0.918
Melt flow index (g/10 min)	1
M_w	84,460
M_n	3,481
MWD	24.26

Linear Low Density Polyethylene obtained by liquid or gas phase polymerization by virtue of ethylene and α-olefins such as butene-1, hexene-1or octene-1. It was found that LLDPE resins had broad molecular weight. The M_w, M_n and MWD of LLDPE were characterized as shown in Table 4.1 (see also Appendix B)

4.1.1.2 Natural Rubber (NR)

Table 4.2 Characteristics of NR.

Characteristics	Value
Density (g/cm^3)	0.900
Melt flow index (g/10 min)	–
M_w	125,000
M_n	22,241
MWD	5.62

Natural Rubber obtained from the latex produced by tree *Hevea braseliensis*. M_w, M_n and MWD of NR can be varied dependent on season of trapping, age of tree, and process condition during latex coagulation. In this work, it was found that masticating process could reduce the M_w, M_n and MWD of NR. The mechanism for reducing the molecular weight of NR could be seen in section 2.3. From Table 4.2 reveals M_w, M_n and MWD of NR at milling time 10 minute (see also Appendix B).

4.1.1.3 LLDPE/NR Blends

Table 4.3 Characteristics of LLDPE/NR blends.

Samples	MFI (g/10 min)	M_w	M_n	MWD
90/10/0	0.949	85,427	2,733	31.25
90/10/1	0.469	84,178	2,837	29.67
90/10/3	0.265	91,235	3,709	24.60
80/20/0	0.897	87,255	2,467	35.60
80/20/1	0.418	91,573	3,047	30.05
80/20/3	0.173	90,295	3,271	27.60
80/20/5	0.153	117,164	4,094	24.96
70/30/0	0.7677	10,852	3,012	36.02
70/30/1	0.6613	114,039	3,023	32.72
70/30/3	0.1414	114,004	3,400	35.53
70/30/5	0.0883	138,130	4,297	32.14

The M_w, M_n and MWD of the blends were characterized as shown in Table 4.3. It was found that the maleic anhydride (MA) acts as a compatibilizer playing an important role to the molecular parameters of blends. M_w and M_n of the blends increased when wt% of MA increased. The mechanism of MA reacted with LLDPE and NR is proposed by P. Limsila, (1999). It seems to be that MA formed graft copolymer of NR-MA-LLDPE *in-situ* during melt mixing. When wt% of MA increased in the system, the formation of graft copolymer of NR-MA-LLDPE increased resulting in the enhancement of the efficiency of graft copolymer to act as a compatibilizer for LLDPE/NR blends. Thus, an increase of molecular weight of the blends would be obtained. Matos and Favis found the similar results that they blended LLDPE and PS by using SEBS as a compatibilizer. They inferred that one side of SEBS functionalized with LLDPE, the other side functionalized with PS and then formed LLDPE-SEBS-PS graft copolymer. When the amount of SEBS increased so, the formation of copolymer increased resulting in an enhancement the compatibility and also the high molecular weight of the blends (Matos *et al.*, (1995).

4.2 Processability and Rheological Characteristics

4.2.1 Melt Strength of LLDPE and LLDPE/NR Blends

Table 4.4 Melt viscosity of LLDPE, NR and LLDPE/NR blends.

Materials	Shear viscosity (Pa.s) @ 100 s^{-1}	Shear viscosity (Pa.s) @ 500 s^{-1}	Maximum Draw ratio	Maximum Blow up ratio
LLDPE/NR/MA				
100/0/0	1,368	534	6	5
0/100/0	1,455	521	*	*
90/10/0	1,413	513	5	6
90/10/1	1,593	526	6	6
90/10/3	1,614	546	6	6
80/20/0	1,355	541	*	*
80/20/1	1,438	506	6	5
80/20/3	1,676	584	7	6
80/20/5	1,673	560	7	6
70/30/0	1,530	462	*	*
70/30/1	1,560	544	*	*
70/30/3	1,724	555	*	*
70/30/5	1,809	592	*	*

Note * can not process in blown film extrusion

During the tubular blown film experiment, at fixed blow up ratios, the take up speed was increased until the tubular film was broken, where the tensile force exerted by increasing draw ratio was exceeding a critical value that the tubular bubble could no longer withstand. Such critical force may be termed *ultimate melt strength.* The term melt strength of polymer can be referred to maximum draw ratio and maximum blow up ratio of tubular blown film process (Kwack *et al.*, 1983).

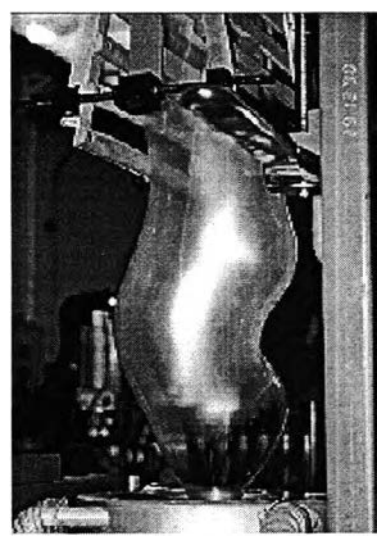

Figure 4.1 Blow instability of LLDPE at BUR 6.

The LLDPE resins exhibited excellent drawability but poor blowability (Figure 4.1). This may be attributed to the absence of long chain branching in LLDPE resins resulting in lower melt strength. From Table 3 addition of NR by 10 wt%, was believed to cause an enhancement of melt strength due to an increase in long chain branching in the matrix of LLDPE. Blow ability of LLDPE with 10 wt% NR was 6 (Figure 4.2) which was greater than that of pure LLDPE (BUR=5).

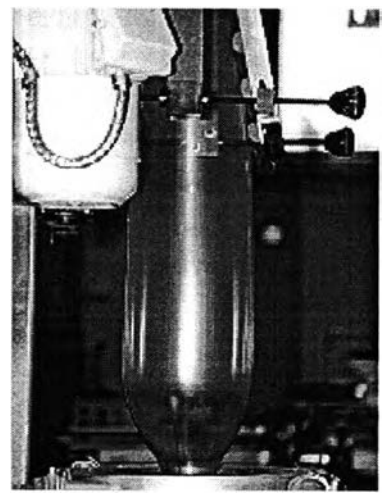

Figure 4.2 Blow stability of LLDPE after introducing 10 wt% of NR at BUR 6.

4.2.2 Melt Viscosity of LLDPE and LLDPE/NR Blends

In this work, the apparent shear viscosity of LLDPE/NR with/without MA was measured at 100 and 500 s^{-1}. These shear rates were assumed to correspond to shear rates found in blown film and chill roll cast film extrusion. Data are shown in Table 4.4. The shear viscosities of the blends are higher than that of LLDPE. It implies that after addition of NR and MA into LLDPE, there is more entanglement present in the blends. So, more shear force is required to disentangle. There was a correlation between shear viscosity and blowability; i. e. it was found that the higher shear viscosity of the blends exhibited better blowability (Utracki *et al.*, (1984).

4.3 Morphology of LLDPE/NR Blends

4.3.1 Effect of Compatibilizer on Morphology of LLDPE/NR Blends

Morphological studies of LLDPE/NR blends are defined for the size, orientation and distribution of the dispersed phase. An important question in this regard is the role of the compatiblizer in reconstituting the microstructure at the interphase. Finally, the origin of improved mechanical performance can be defined by examining the role played by the coexisting domains (continuous phase, dispersed phase and the interphase) in load bearing and in reducing irreversible deformation processes.

The addition of suitably selected compatibilizers to immiscible blends should 1) reduce the interfacial energy of the phases, 2) permit a finer dispersion while mixing, 3) provide a measure of stability against gross phase segregation, and 4) result in improved interfacial adhesion.

Three different types of blends were evaluated, i. e.

1) Blend of LLDPE and NR without any compatibilizing agent
2) Blend of LLDPE and NR with addition of MA
3) Blend of LLDPE and NR with/without comptibilizer under shear effect

The above studies were focused on the 70/30 wt% LLDPE/NR blend.

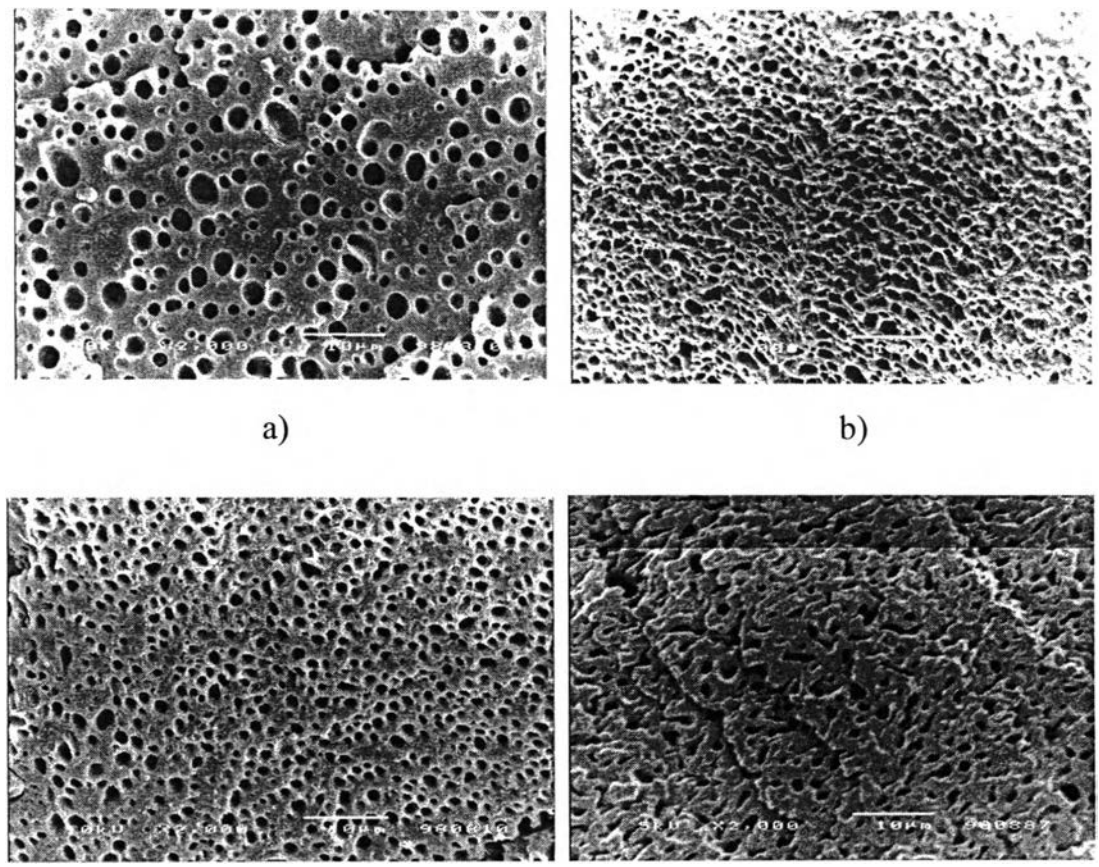

a) b)

c) d)

Figure 4.3 Morphology of LLDPE/NR/MA at composition 70/30; a) 0, b) 1, c) 3, d) 5% MA (magnification 2000X).

The NR dispersed phase shows a spherical shape. Incorporation of MA reduced the averaged NR dispersed phase size (see Figure 4.3a-d), e. g. from 1.48 to 0.98 μm (see Appendix C). Here, uniform dispersion as well as distribution of the dispersed phases can be observed. This reduction in particle size with the addition of compatibilizer was possibly due to the reduction in interfacial tension between the LLDPE matrix and NR dispersed phase. Increasing the MA proportion to 5 wt% reduced the dispersed phase size of NR

further to 0.8 μm because of better compatibilization, as shown in Figures 4.3d. An increased surface area of the dispersed phase morphology and an effective compatibilization was responsible for the increased adhesion strength between the blend components. Thus, 5 wt% of MA compatibilizers was considered to be the optimum level for compatibilizing the 70/30 wt% LLDPE/NR blends.

4.3.2 Effect of Shear Rate on Morphology of LLDPE/NR Blends

The deformation field in compounding or processing equipment is usually complex, leading to a multitude of morphological forms. In this part the effects of a simple deformation field, shear or extensional will be considered. The analysis of morphological development during process, especially at the die becomes more important. It was found that the morphology of the extrudate might vary from the core to the surface depending on the blend type and processing conditions used (Zloczower *et al.*, 1994).

In our work the morphology from capillary rheometer at different shear rates ranging from 40-250 s^{-1} were examined and the morphology at core was used to represent the morphology that might be occurring in the real processing (see Figures 4.4-4.7).

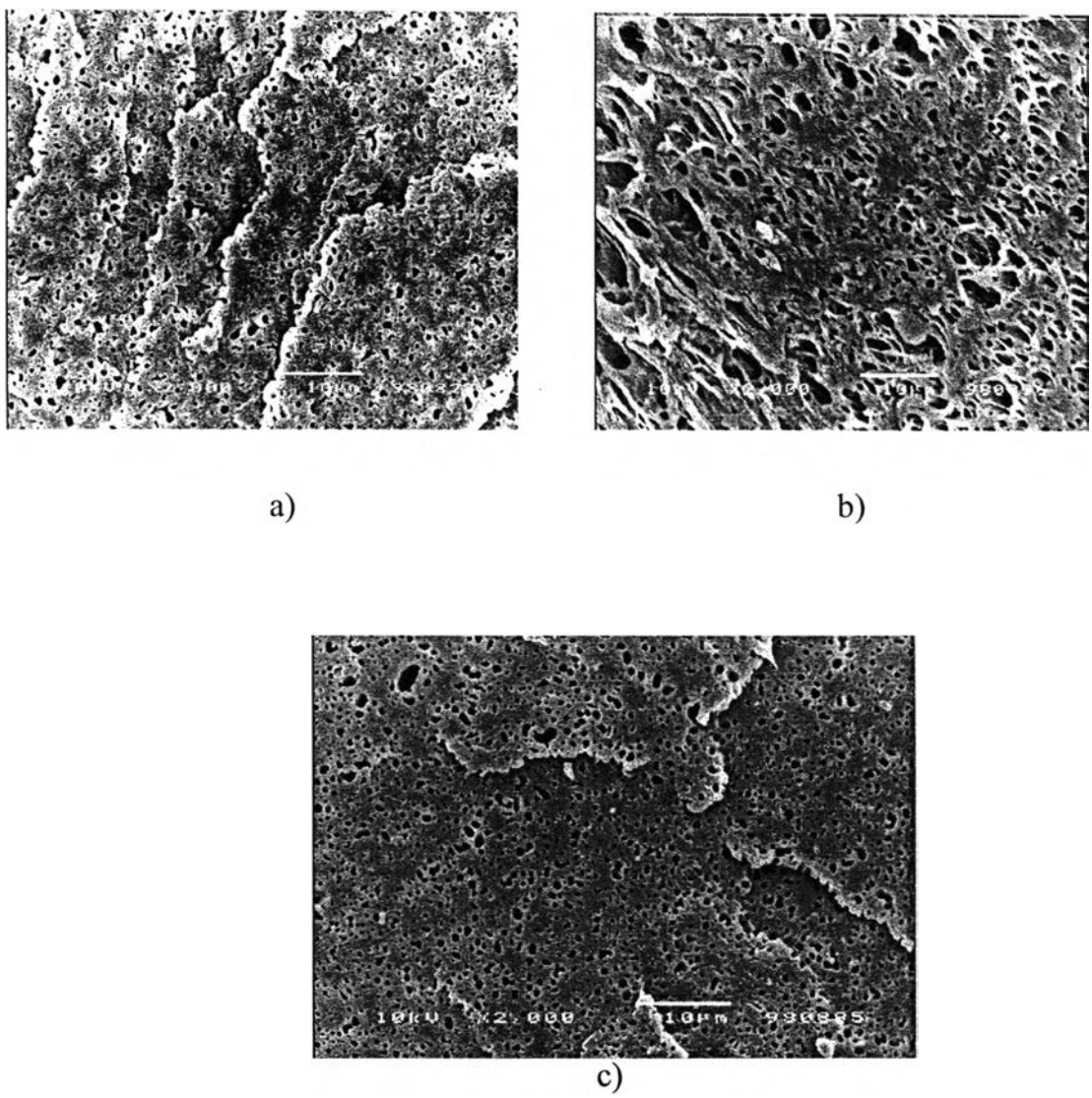

Figure 4.4 Morphology of LLDPE/NR /MA at 70/30/0%; a) shear rate 46.54 s^{-1}, b) shear rate 139.60 s^{-1}, c) shear rate 232.70 s^{-1} (magnification 2000X).

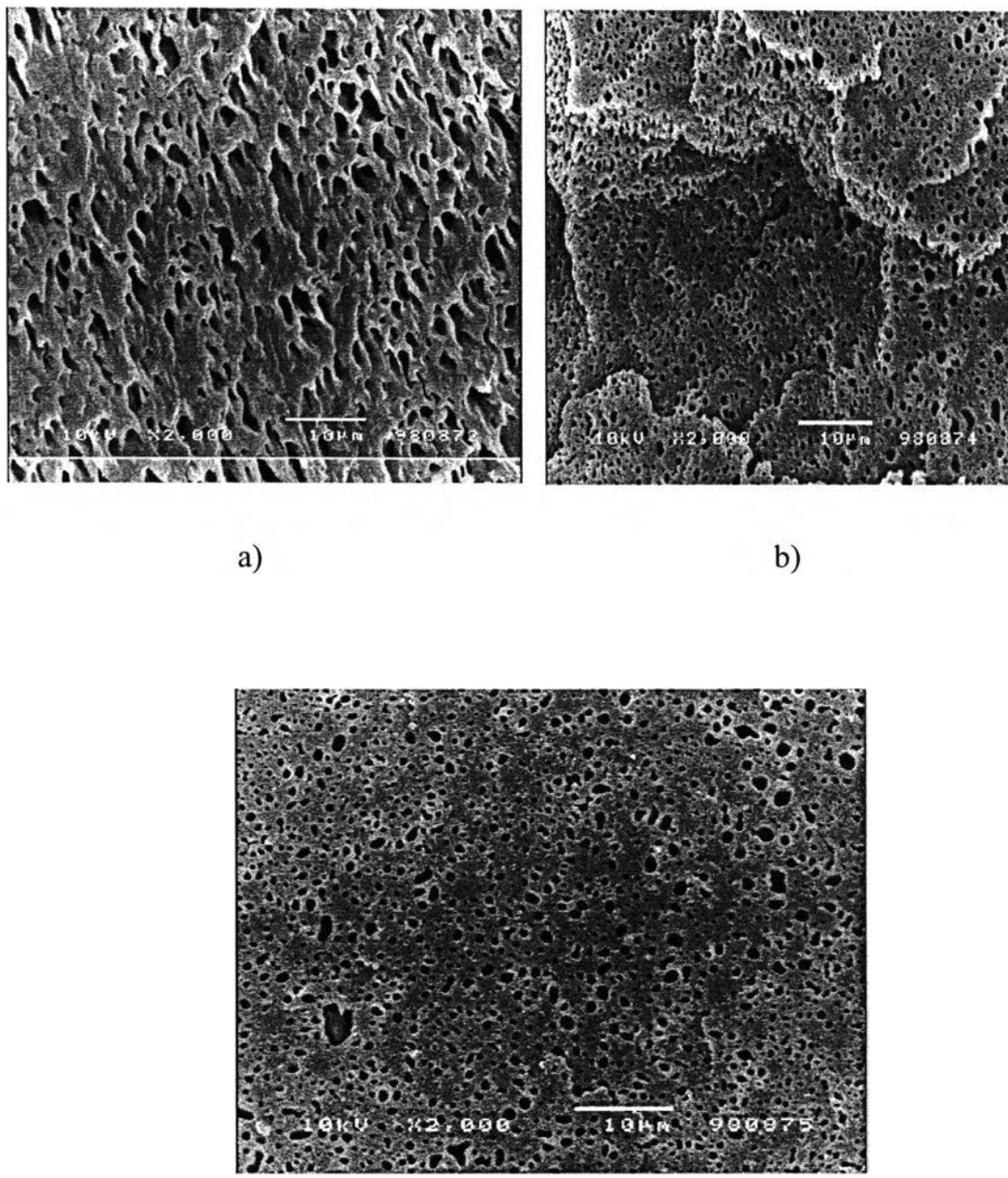

a) b)

c)

Figure 4.5 Morphology of LLDPE/NR /MA at 70/30/1%; a) shear rate 40.70 s^{-1}, b) shear rate 122.10 s^{-1}, c) shear rate 203.60 s^{-1} (magnification 2000X).

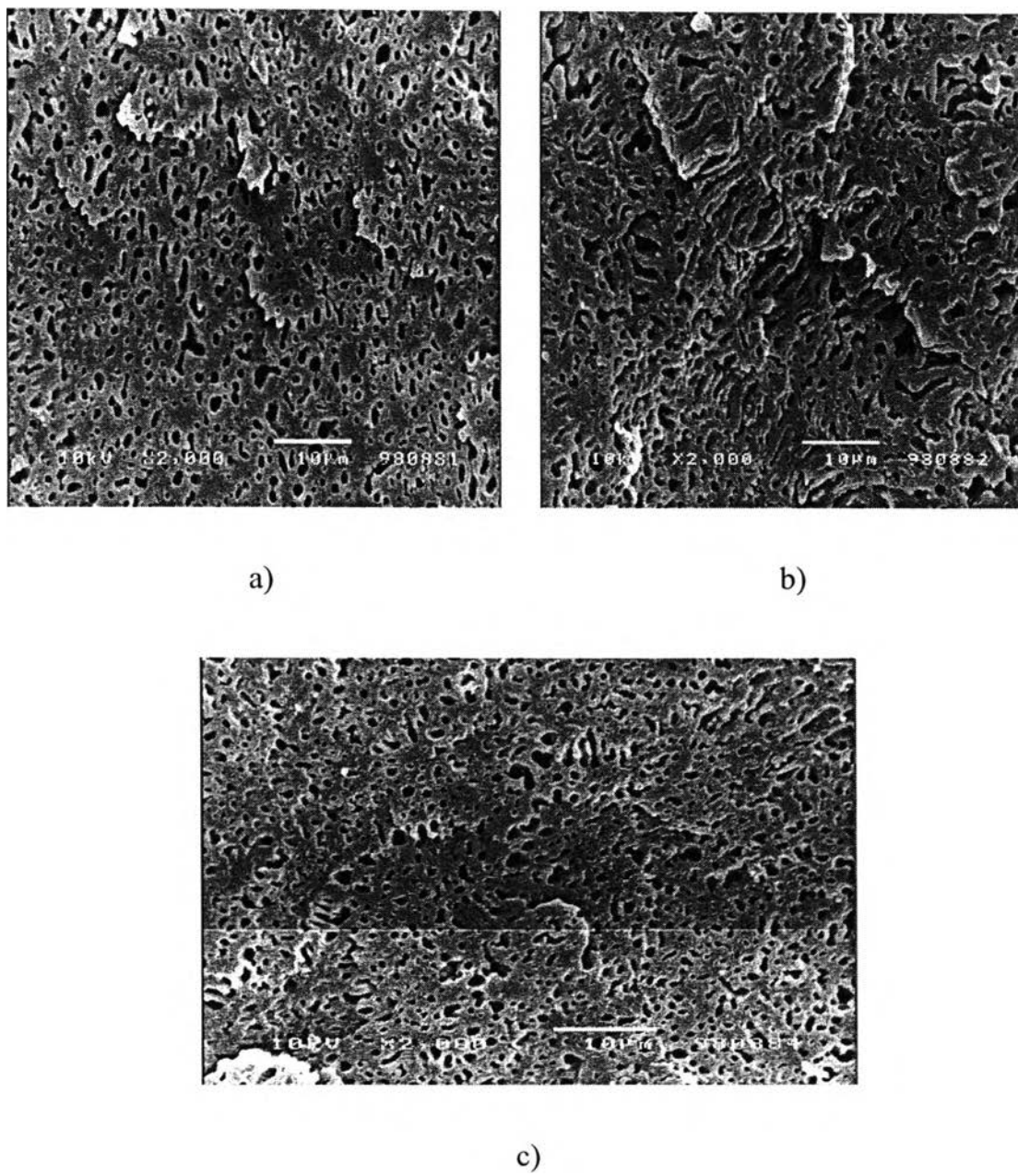

Figure 4.6 Morphology of LLDPE/NR /MA at 70/30/3%; a) shear rate 43.12 s^{-1}, b) shear rate 129.40 s^{-1}, c) shear rate 215.60 s^{-1} (magnification 2000X).

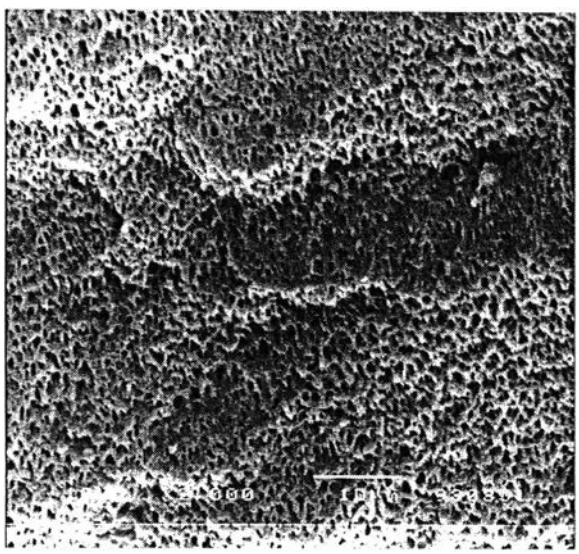

a)

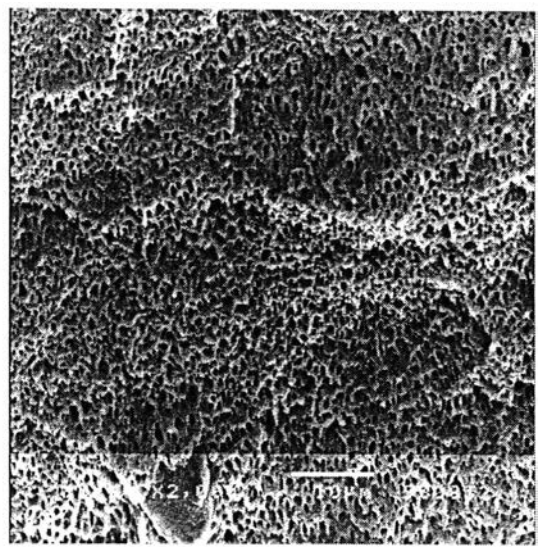

b)

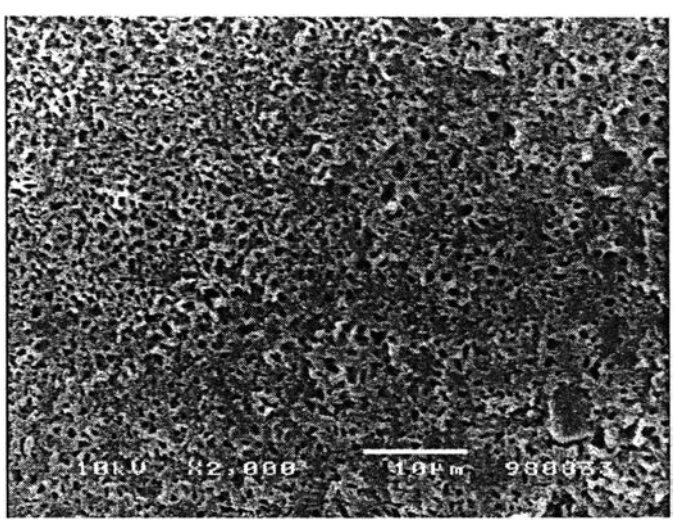

c)

Figure 4.7 Morphology of LLDPE/NR /MA at 70/30/5%; a) shear rate 42.40 s^{-1}, b) shear rate 127.20 s^{-1}, c) shear rate 210.00 s^{-1} (magnification 2000X).

In case of uncompatibilized 70/30 LLDPE/NR blends at shear rate 46.54 s^{-1}, the NR dispersed size was smaller than in the extruded resin (Figure 4.4a by comparison with Figure 4.3a). The dispersed phase became finer with increasing shear rate as evidenced in Figure 4.4c. The results revealed an interesting point, at shear rate 46.54 s^{-1} the shape of NR dispersed phase looked like irregular shape (e. g. oval, sphere and triangle). This was due to NR dispersed phase was broken-down to small droplets. Further increase of shear rate up to 139.60 s^{-1} resulted in rather big and non uniform NR dispersed phase due to the draining of matrix between drops. The film thickness decreased to a critical value and rupture of interface occurred resulting in coalescence (Noolandi *et al.*, 1982). At shear rate 232.70 s^{-1} the NR dispersed phase had a spherical shape; this was due to a competition of coalescence and breakup of NR dispersed phase (Uttandararan *et al.*, 1995). More force applied in the system led to breakup of NR dispersed phase and finer morphology. By adding MA 1 wt% showed that MA was not enough to modify the interface, so a significant change of NR dispersed phase size could be observed (Figure 4.5a-c). Addition of 3 wt% MA modified the morphology. At shear rate 43.12 s^{-1} the NR dispersed phase looked a spherical, while at shear rate 129.40 s^{-1} it looked fibrillar as shown in Figure 4.6a-c. On the other hand, at 5 wt% of MA that we denoted as point of optimum concentration of compatibilizer, the morphology did not change when increasing shear rate from 42.40, 127.20 and 210.00 s^{-1} (Figures 4.7a-c). The averaged NR dispersed size slightly decreased from 0.68, 0.66, 0.65 μm respectively.

4.4 Thermal Properties of LLDPE, NR and LLDPE/NR Blends

The melting (T_m) and glass transition temperature (T_g) of LLDPE, NR and LLDPE blends with/without MA were determined by DSC.

4.4.1 Effect of NR on Melting Temperature (T_m) and Degree Crystallinity of LLDPE

The ability of material to crystallize is determined by the regularity of its molecular structure. It was found that NR caused a decreasing of T_m in LLDPE/NR blends. A lower degree of crystallinity was expected. LLDPE exhibited degree crystallinity of about 33%, while addition of 10, 20 and 30 wt% NR caused a decrease of degree crystallinity to 20% which are shown in Table 4.5.

Table 4.5 Degree of crystallinity of LLDPE and LLDPE/NR blends

Compositions	Degree of a crystallinity*	T_m
LLDPE	33.81±1	123±1
90/10	31.16±2	121±2
80/20	28.74±1	121±1
70/30	26.16±1.5	120±1

*ΔH_{f100} = *Heat of fusion for 100% crystallinity of LLDPE (299.1 J/g)*

4.4.2 Effect of MA on Glass Transition Temperature (T_g) of LLDPE/NR Blends

In the case of LLDPE/NR blends, it was found that LLDPE and NR were incompatible in nature. MA was added as a compatibilizer during blending to react with pure component. For example, at composition 80/20 wt% without MA two T_gs were exhibited at -21 and -48^{0}C corresponding to T_g of LLDPE and NR. In the addition of 1 wt% MA, T_g was shifted and become closed together but there still were two T_gs. Further addition upto 5 wt% a single T_g was observed lying between T_g of LLDPE and NR. This indicated that at 5 wt% MA added, the miscibility of LLDPE/NR blends at composition 80/20 wt% was achieved. Similar trend was observed for blend composition of 70/30 wt%. It is interesting that the film LLDPE/NR samples of composition 90/10 wt% with and without MA show a single T_g indicating the compatibility of LLDPE and NR. Glass transition temperatures for compositions 90/10 and 70/30 wt% are shown in Table 4.6.

Table 4.6 Glass transition temperatures (T_g) of LLDPE, NR and LLDPE/NR blends.

Compositions	T_{g1}	T_{g2}
LLDPE	-21	-
NR	-62	-
90/10/0	-33	-
90/10/1	-40	-
90/10/3	-60	-
80/20/0	-21	-48
80/20/1	-25	-45
80/20/3	-37	-45
80/20/5	-44	-
70/30/0	-43	-64
70/30/1	-41	-55
70/30/3	-42	-55
70/30/5	-54	-

4.5 Molecular Orientation

4.5.1 Infrared Dichroism

The orientation of macromolecules play an important role in determining their performance, mechanical and optical characteristics. Molecular orientation can be determined by FTIR, optical polarized microscope and XRD. In this study, FTIR or dichroism and birefringence (polarized microscope) were employed. The molecular orientation of LLDPE/NR blends induced by uniaxial stretching and biaxial stretching was investigated.

4.5.1.1 Effect of Process Variables BUR and DR for LLDPE and LLDPE/NR Blend Films Produced by Blown Film Process

Blown film process was also developed to produce biaxial orientation. The orientation function (f) was plotted versus draw ratio as shown in Figure 4.8.

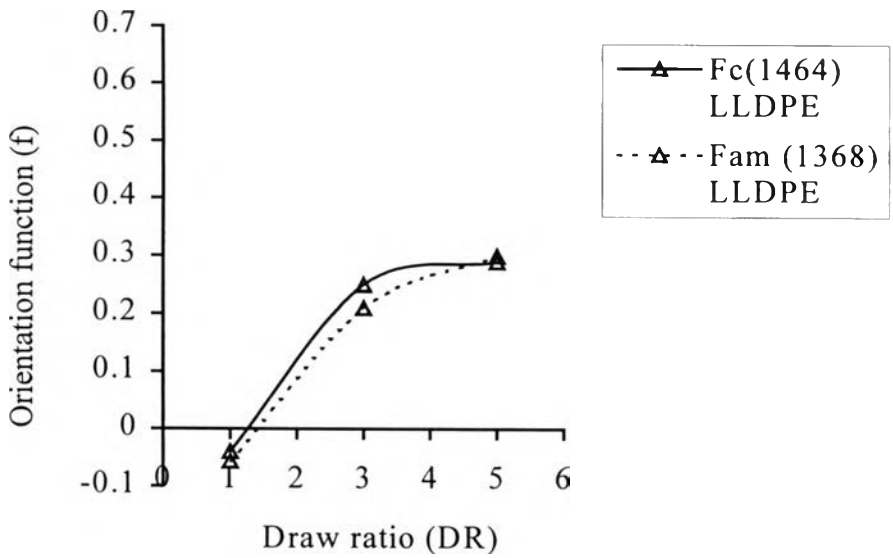

Figure 4.8 Crystalline (f_c) and amorphous (f_{am}) orientation functions of LLDPE blown films at BUR 3 and DR 1, 3 and 5.

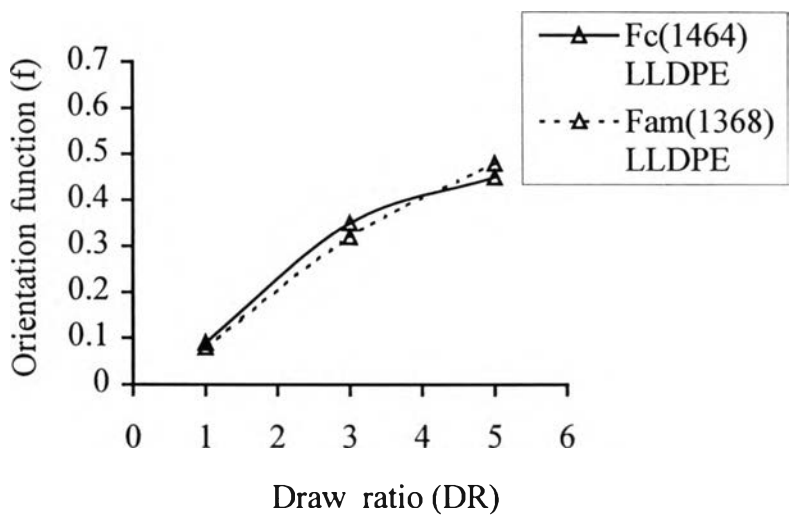

Figure 4.9 Crystalline (f_c) and amorphous (f_{am}) orientation functions of LLDPE blown films at BUR 5 and DR 1, 3 and 5.

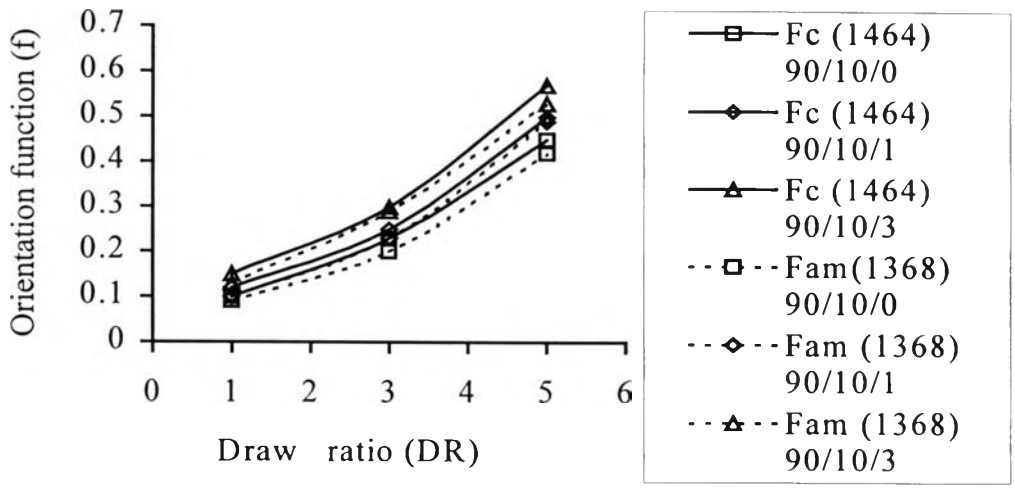

Figure 4.10 Crystalline (f_c) and amorphous (f_{am}) orientation functions of LLDPE/NR blown films at composition 90/10 wt% at BUR 3 and DR 1, 3 and 5.

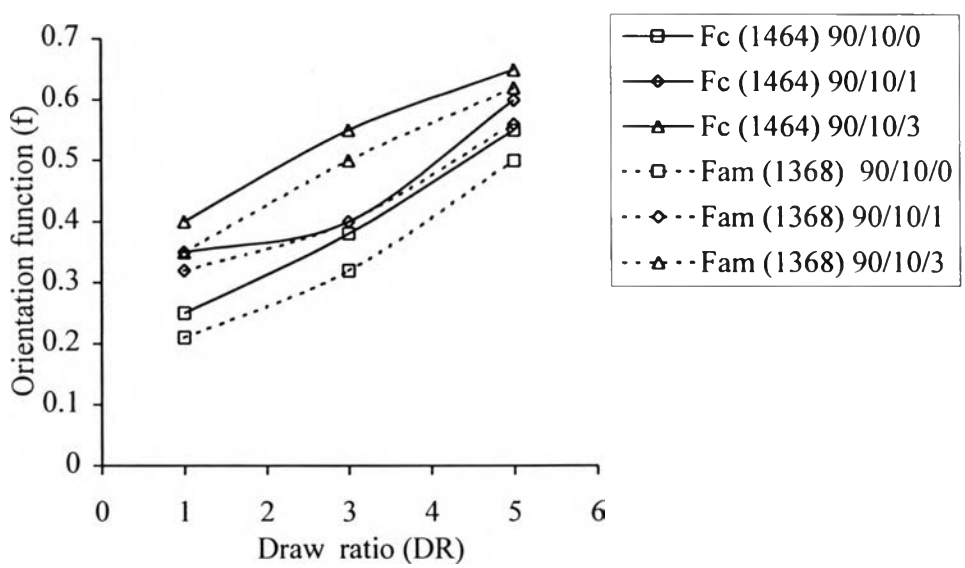

Figure 4.11 Crystalline (f_c) and amorphous (f_{am}) orientation functions of LLDPE/NR blown films at composition 90/10 wt% at BUR 5 and DR 1, 3 and 5.

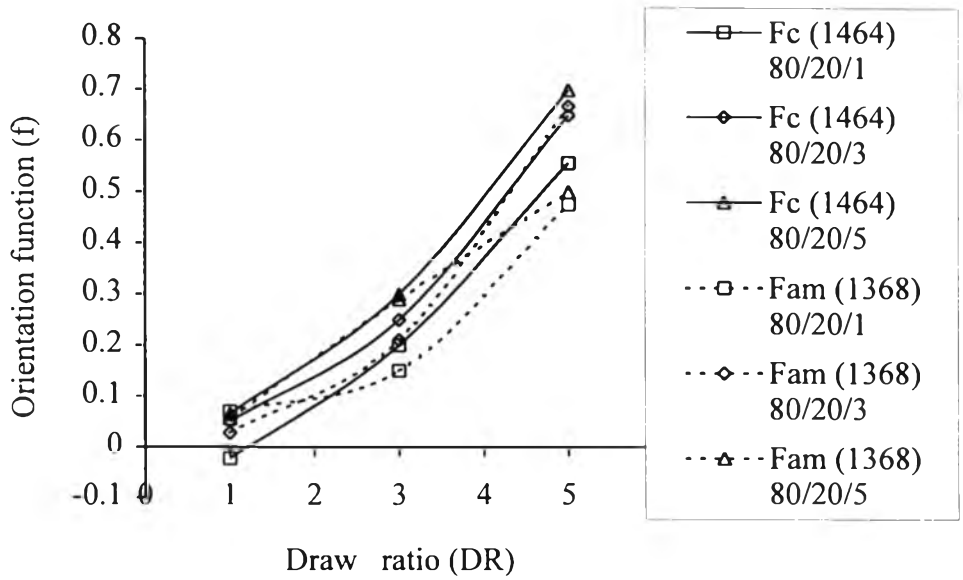

Figure 4.12 Crystalline (f_c) and amorphous (f_{am}) orientation functions of LLDPE/NR blown films at composition 80/20 wt% at BUR 3 and DR 1, 3 and 5.

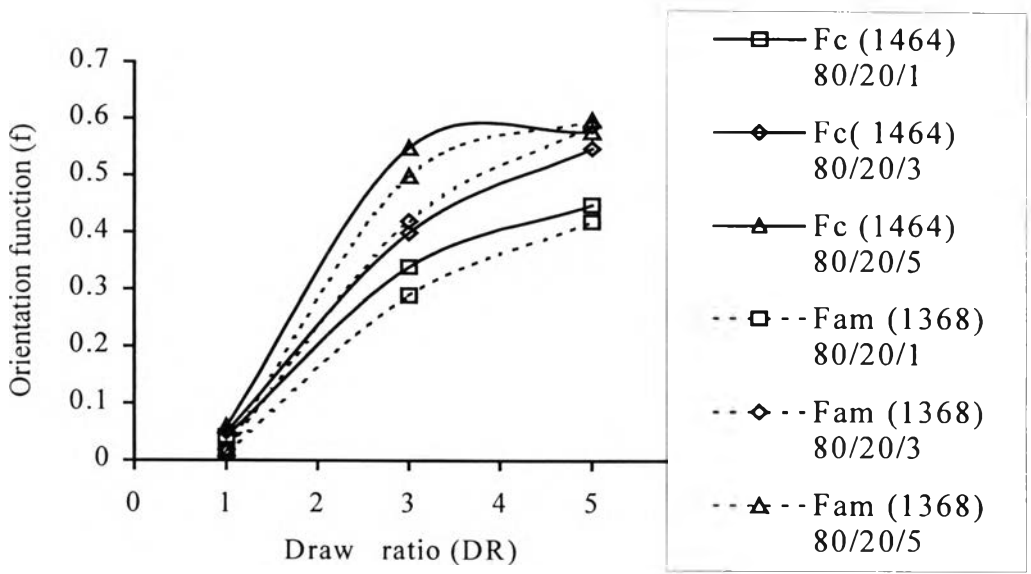

Figure 4.13 Crystalline (f_c) and amorphous (f_{am}) orientation functions of LLDPE/NR blown films at composition 80/20 wt% at BUR 5 and DR 1, 3 and 5.

Blown film process was also developed to produce biaxial orientation. At fixed BUR 3 and DR 1, it was clearly seen that the crystalline orientation (f_c) and amorphous orientation (f_{am}) were slightly negative as shown in Figure 4.8. This was due to higher molecular mobility at elevated temperatures (Pezzutti *et al.*, 1985). The LLDPE films were generally broken at draw ratio above 5, which corresponded to maximum or *ultimate melt strength* of LLDPE. The crystalline orientation function increased rapidly upon extension and reached a value about 0.3 at draw ratio 5 (see Appendix D). This indicated a very high segmental orientation of the crystalline structure of LLDPE, which was aligned parallel to the stretching direction. On the other hand f_{am} was lower than the crystalline orientation. The f_{am} had a value around

0.2 at draw ratio 3 after that increased to 0.3 at draw ratio 5. The amorphous segments resided in the interlamellar region existed in various forms: tie chains, cilia, loops and unattached chains as shown in Figure 4.18 (Groeninckx *et al.*, 1993). Generally the tie chains interconnected by the crystal blocks was expected to orient more than cilia, loops and unattached chains that also relaxed more rapidly. At BUR 5, increasing speed of nip roll until reached DR 5, f_c and f_{am} were 0.5 (Figure 4.9). It implied that at BUR 5 and DR 5 molecules oriented in both MD and TD. So we can conclude that orientation function appeared to be very sensitive to process variable.

4.5.1.2 Molecular Orientation of Film Produced from Chill Roll Cast Film Process.

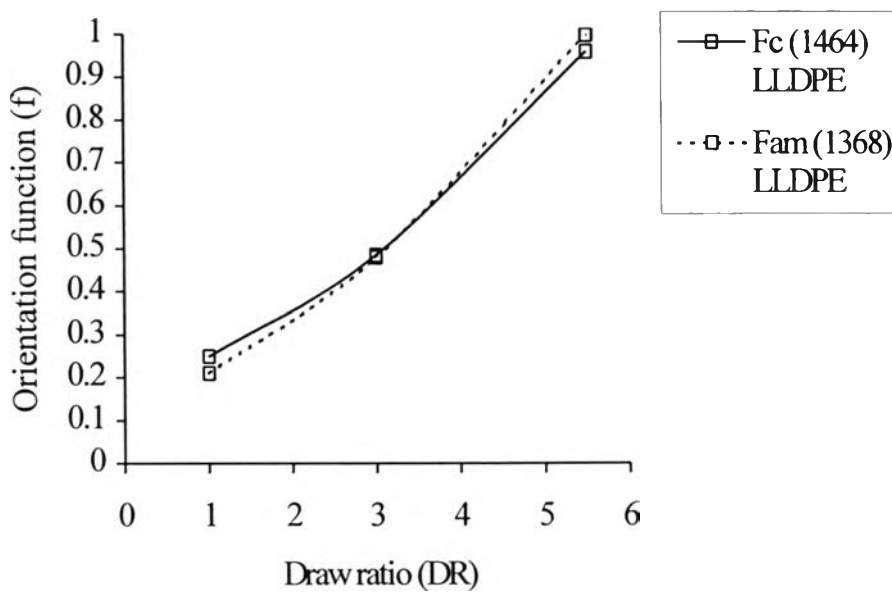

Figure 4.14 Crystalline (f_c) and amorphous (f_{am}) orientation functions of LLDPE at DR 1, 3 and 5.5.

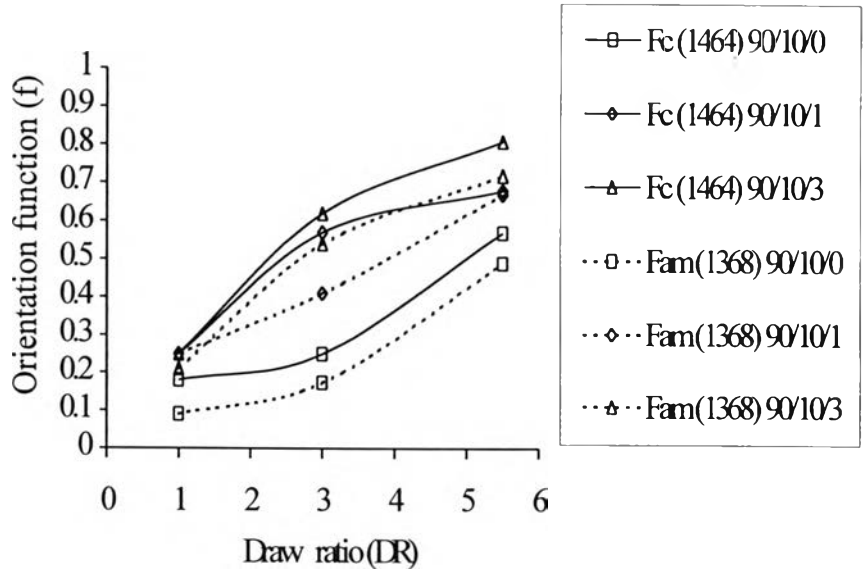

Figure 4.15 Crystalline (F_c) and amorphous (F_{am}) orientation functions of LLDPE/NR blown films at composition 90/10 wt% at DR 1, 3 and 5.5.

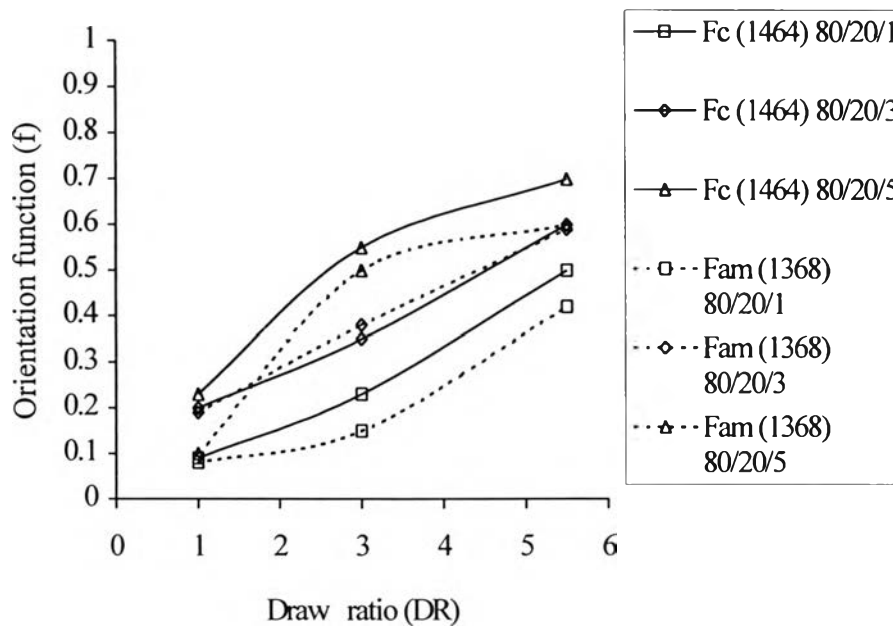

Figure 4.16 Crystalline (f_c) and amorphous (f_{am}) orientation functions of LLDPE/NR blown films at composition 80/20 wt% at DR 1, 3 and 5.5.

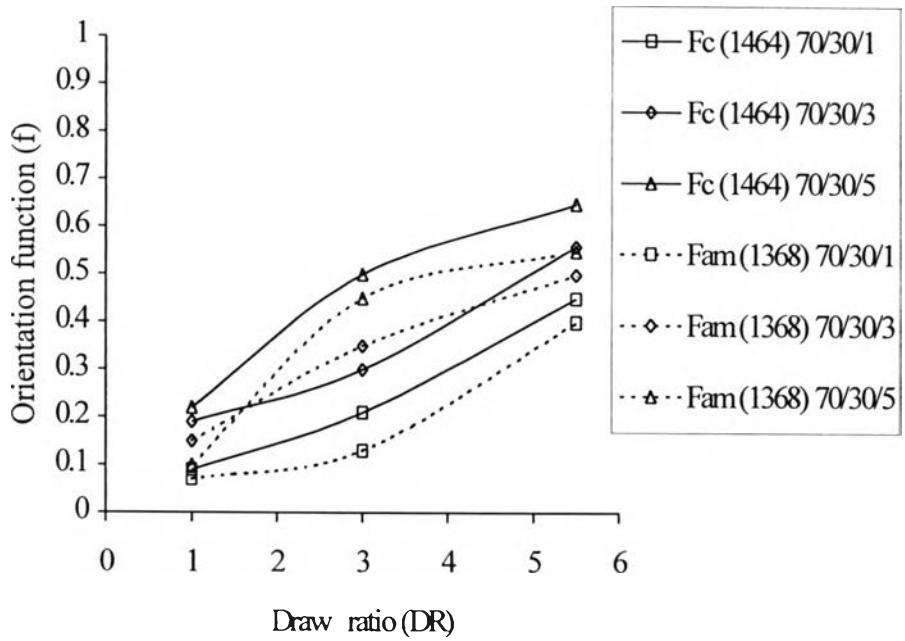

Figure 4.17 Crystalline (f_c) and amorphous (f_{am}) orientation functions of LLDPE/NR blown films at composition 70/30 wt% at DR 1, 3 and 5.5.

The f_c and f_{am} of LLDPE films from the chill roll cast film process are shown in Figure 4.14. It was seen clearly that both f_c and f_{am} were increased with increasing DR. It was noticed that at DR 5.5 both f_c and f_{am} of LLDPE and the blends exhibited value around 0.6-1.0. It implied that at high DR molecules tended to orient mainly in MD resulting in increasing strength of LLDPE in MD rather than that in TD (see in part 4.6). The f_c and f_{am} of LLDPE/NR blend films at composition 90/10, 80/20 and 70/30 wt% are shown in Figures 4.15-4.17.

4.5.1.3 Effect of NR and MA Content on Crystalline (f_c) and Amorphous Orientation (f_{am}) of LLDPE Phase in LLDPE/NR Blends

The f_c and f_{am} of LLDPE phase in LLDPE/NR blends from blown film process at composition 90/10, 80/20 and 70/30 wt% are shown in Figures 4.10-4.17 for both blown films and cast films. It was already known from the previous part that NR had a significant effect on the crystallization behavior of LLDPE. The crystalline block of the blend was volume filling and the amorphous layers (interlamellar spacing) were increased as the content of NR increased. It was assumed that after introducing NR to LLDPE without MA compatibilizer, the amorphous segments of NR behaved like unattached chains in the system. During the drawing process unattached chains that relaxed rapidly tended to recover to the initial state relatively faster than the attached chains, resulting in decreasing orientation. The f_c and f_{am} increased with increasing MA content. For example, Figure 4.11 f_c and f_{am} of LLDPE/NR blends at composition 90/10 wt% without MA had value around 0.45 at DR 5. By addition of 1 and 3 wt% MA, f_c and f_{am} increased to 0.6. This indicated that MA played a significant role in the orientation of both crystalline and amorphous segments. This was due to MA performing as compatibilizer to connect NR and LLDPE. During the drawing process as in blown film and chill roll cast film processes, stress could be transferred between interface nicely resulting in a very high segmental orientation. Moreover, amorphous phase of NR and LLDPE could be possibly connected with each other by tie chains which could not relax easily during the solidification process. The f_c and f_{am} for composition 80/20 and 70/30 wt% showed the similar results.

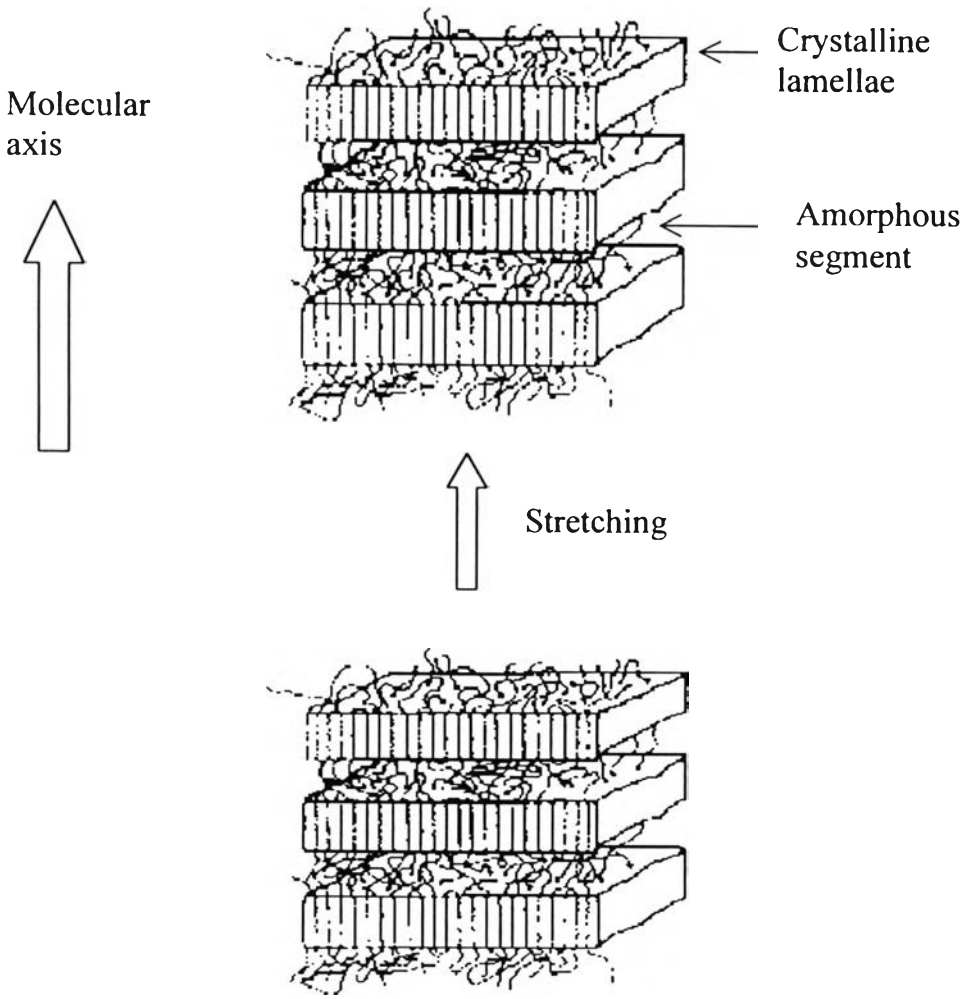

Figure 4.18 Sketch of basic semicrystalline structure, the crystalline lamellae connected with amorphous segments by tie chains.

4.5.1.4 Comparing Biaxial and Uniaxial Molecular Orientation between Blown Film and Chill Roll Cast Film Process

The main parameters in the correlation of orientation in blown film and chill roll cast film affecting molecular orientation are the cooling conditions of the extrusion line, the deformation process and the stress relaxation behavior of the polymer (Groeninckx *et al.*, 1993).

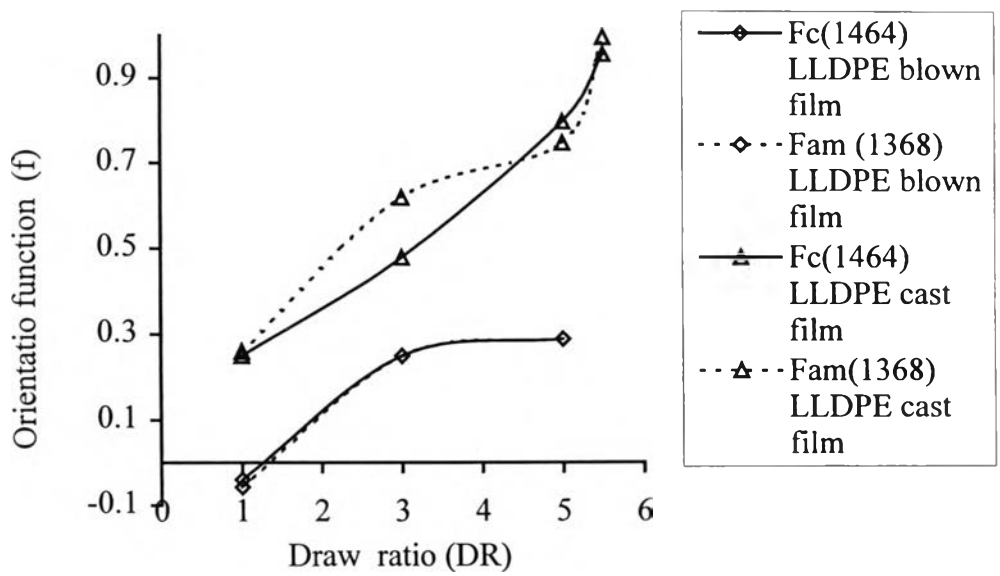

Figure 4.19 Crystalline (f_c) and amorphous (f_{am}) orientation functions of LLDPE blown films at BUR 3 and chill roll cast film processes.

Figure 4.19 shows clearly that both f_c and f_{am} of the film produced by a chill roll cast film process are much higher than that from a blown film process. This was due to three main factors. First in the chill roll process; the polymer melt was cooled rapidly by chill roll drum and stretched at the same time. So the molecules do not have enough time to relax to an

unoriented state resulting in higher orientation (Goreninckx *et al.*, 1993). On the other hand, in the blown film process polymer melt was extruded from an annular die and molecular orientation induced between the die and frost lines. In this step the distance from die to frost line was important because the longer frost line caused more molecular orientation. The second factor was cold drawing which is more effective to orient molecules than melt drawing. Finally, in the chill roll process uniaxial stress was exerted but in the blown film biaxial stress was dominant (Brydson *et al.*, 1995).

4.5.2 Effect of Process Variables on LLDPE Blown Film Determined by Birefringence

Birefringence was used as a method to characterize the molecular orientation in the stretched films. C-axis along the backbone was chosen as a principle axis that was parallel to stretch direction. Newton chart was used extensively in this work. The color appearance based on the difference in the principal refractive indices, which were lined parallel and perpendicular to the stretched direction for uniaxial and biaxial stretched specimens. Birefringence was calculated as following.

$$\Delta n = \frac{R}{t} \tag{4.1}$$

Where Δn is birefringence, R is retardation and t is thickness of films.

Retardation of sample can be defined as

$$R_{(sample)} + R_{(reference)} = R_{(\lambda)} \tag{4.2}$$

$$R_{(sample)} + R_{(reference)} = R_{(\lambda/4)} \tag{4.3}$$

And hence, sample retardation can be averaged from two measurement by using lamda (λ) and quarter lamda (λ/4) plate. Once the sample retardation is known as well as the sample thickness, equation (4.2) can be employed to calculate for birefringence.

a) cross polar (H)

b) λ

Figure 4.20 Optical polarizing microscope of fully extended chains (magnification 400X).

c) λ/4

Figure 4.21 Optical polarizing microscope of fully extended chains (magnification 400X).

From Figures 4.20-21, it was seen that film exhibited various color under polarized light. This was due to 2 factors: first was a difference of molecular orientation in any region caused a different reflective index in film and the last was stretching causing thickness nonuniformity of films. Nevertheless, it was noticed that (λ/4) plate was inserted between cross-polar, the color was shifted up Newton' scale. So, a positive sign was assigned for birefringence value.

Table 4.7 Birefringence of LLDPE films from blown film at BUR 3.

Draw ratio (DR)	Thickness (μm)	Birefringence
1	60	+0.014
3	50	+0.015
5	33	+0.015

Table 4.8 Birefringence of LLDPE films from blown film at BUR 5.

Draw ratio (DR)	Thickness (μm)	Birefringence
1	50	+0.014
3	45	+0.015
5	30	+0.015

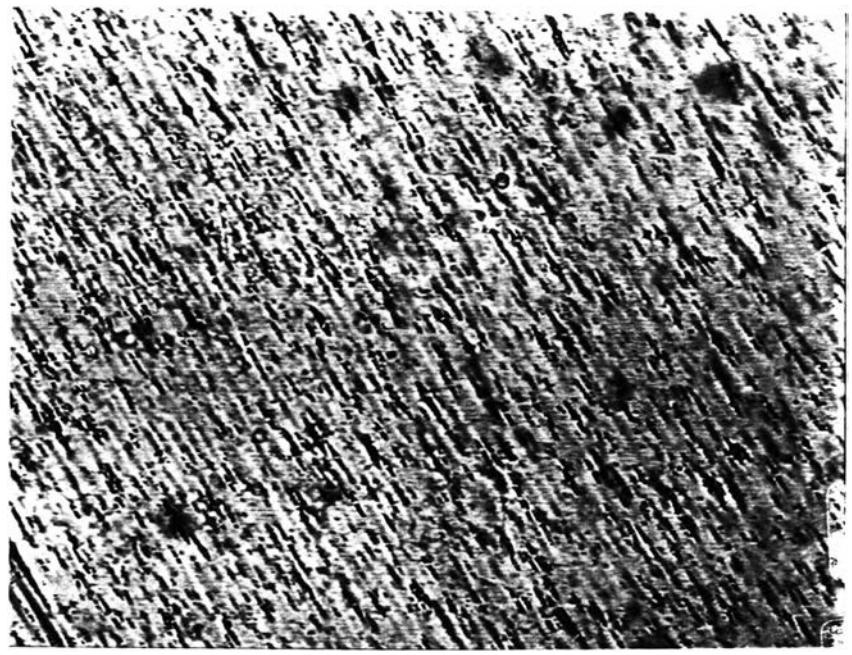

a) λ

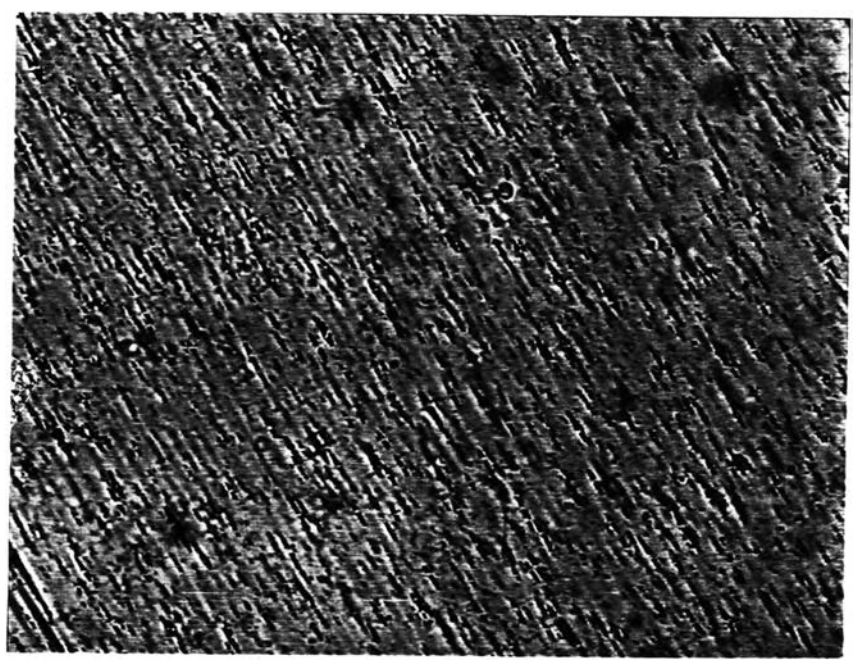

b) λ/4

Figure 4.22 Optical polarizing microscope of LLDPE film from blown film at BUR 3.

From Tables 4.8, It can be seen that birefringence value for LLDPE film at different DR or BUR, no different values were observed while there was shown large difference molecular orientation between BUR 3 and BUR 5 by dicroic ratio. So it could be drawn that for this work birefringence technique was not useful for characterization molecular orientation quantitatively due to its rough scale.

Another important information obtained from birefringence is the stress exerted on the material according to the equation below.

$$\Delta n = C \Delta \sigma \tag{4.5}$$

Where C is the optical constant, $\Delta\sigma$ is the stress difference between two principle axes. Therefore, there is increase of difference stress in two principle axes. From results in Tables 4.7-4.8, stress difference increased with increasing draw ratio.

4.6 Mechanical Properties

LLDPE and LLDPE/NR blend films were prepared using the Betol single screw blown film and Collin chill roll cast film extrusion. Specimens were cut from these films to use for the mechanical properties test. The film thickness are shown in Tables 4.9-4.11. It is noted that samples produced by blown film extrusion at BUR 3 and DR 3 was the same thickness as those produced by chill roll casting at DR 5.5. These two samples with the same thickness show difference mechanical properties as shown later.

Table 4.9 Thickness of LLDPE and LLDPE/NR blend films from blown film process at BUR 3.

Sample	Thickness (μm) DR 3	Thickness (μm) DR 5
LLDPE	40	30
90/10/0	41	32
90/10/1	40	30
90/10/3	42	31
80/20/1	40	32
80/20/3	40	30
80/20/5	40	30

Table 4.10 Thickness of LLDPE and LLDPE/NR blend films from blown film process at BUR 5.

Sample	Thickness (μm)DR 3	Thickness (μm) DR 5
LLDPE	30	25
90/10/0	32	25
90/10/1	32	25
90/10/3	30	25
80/20/1	30	25
80/20/3	30	26
80/20/5	30	26

Table 4.11 Thickness of LLDPE and LLDPE/NR blend films from chill roll cast film process.

Sample	Thickness (μm) DR 1	Thickness (μm) DR 3	Thickness (μm) DR 5.5
LLDPE	60	50	40
90/10/0	60	50	40
90/10/1	62	55	45
90/10/3	60	50	40
80/20/1	60	50	45
80/20/3	60	50	40
80/20/5	60	50	42
70/30/1	60	53	40
70/30/3	60	50	40
70/30/5	60	50	40

4.6.1 Tensile Strength at Break

4.6.1.1 Effect of Process Variables BUR and DR in Blown Film Process on Tensile Strength at Break of LLDPE and LLDPE/NR Blend Films

Tensile strength at break of biaxially oriented films in MD and TD of LLDPE are shown in Figures 4.23 and 4.24.

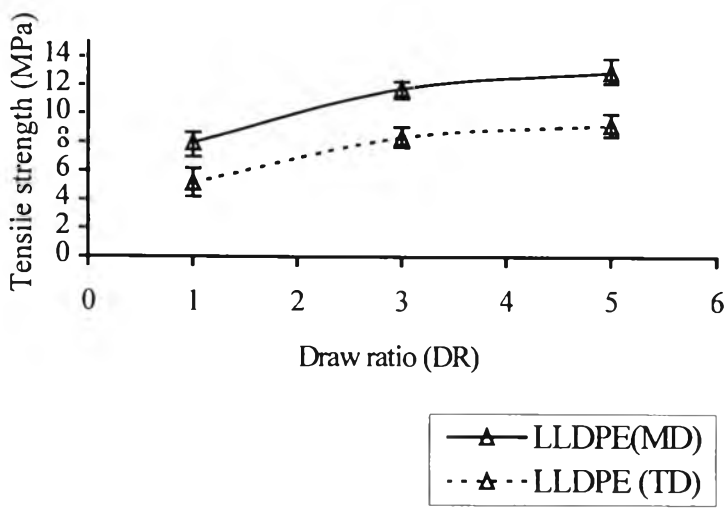

Figure 4.23 Tensile strength at break for LLDPE blown films in MD and TD at BUR 3, DR 1, 3 and 5.

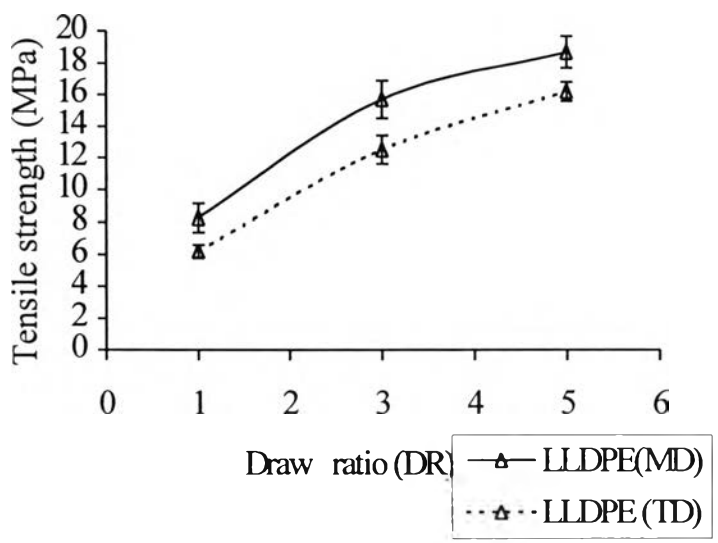

Figure 4.24 Tensile strength at break for LLDPE blown films in MD and TD at BUR 5, DR 1, 3 and 5.

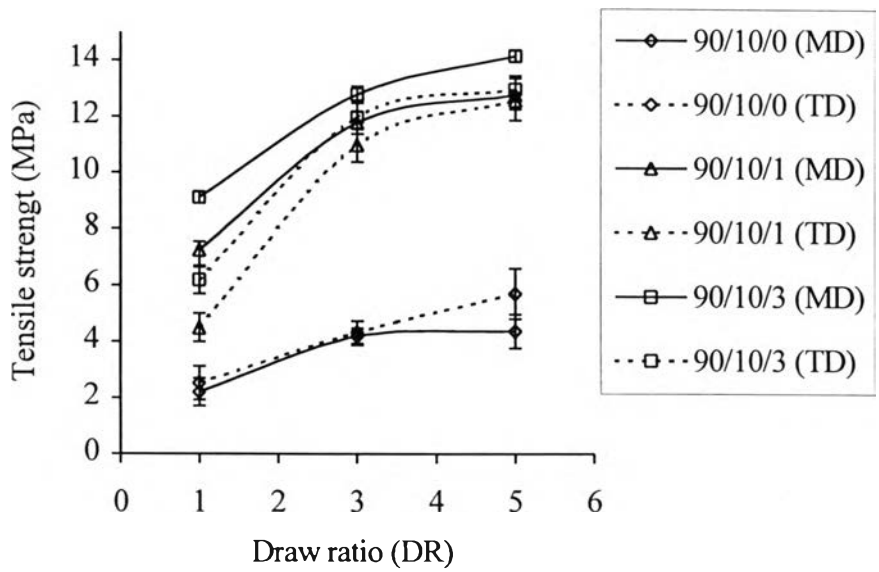

Figure 4.25 Tensile strength at break for LLDPE/NR blown films at composition 90/10 wt% in MD and TD at BUR 3, DR 1, 3 and 5.

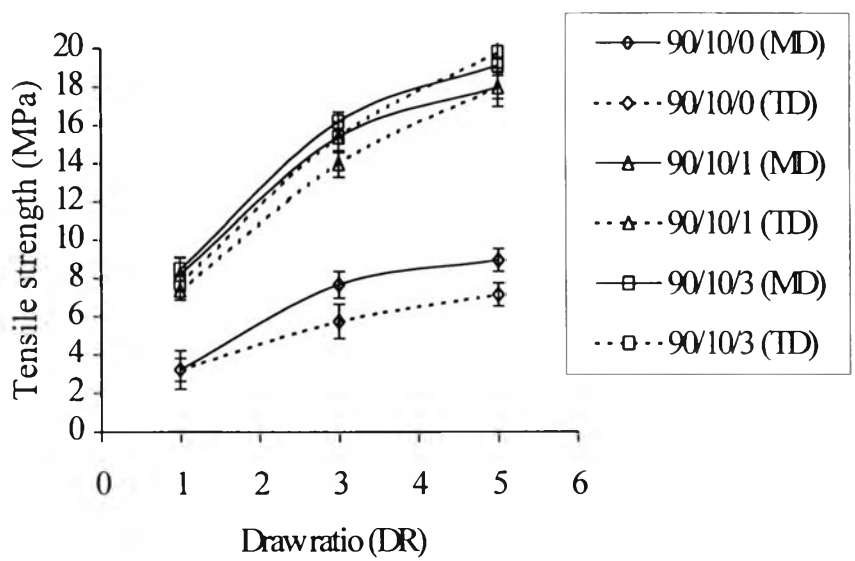

Figure 4.26 Tensile strength at break for LLDPE/NR blown films at composition 90/10 wt% in MD and TD at BUR 5, DR 1, 3 and 5.

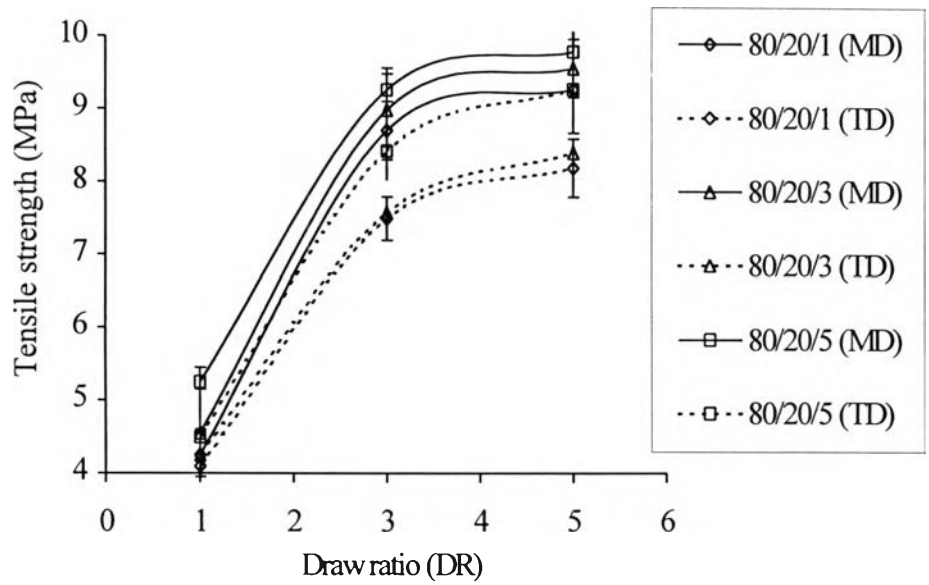

Figure 4.27 Tensile strength at break for LLDPE/NR blown films at composition 80/20 wt% in MD and TD at BUR 3, DR 1, 3 and 5.

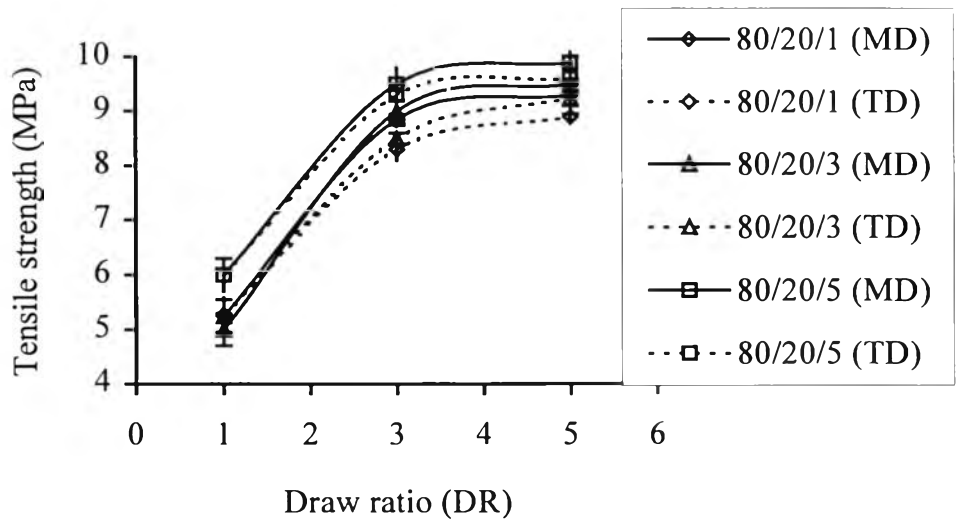

Figure 4.28 Tensile strength at break for LLDPE/NR blown films at composition 80/20 wt% in MD and TD at BUR 5, DR 1, 3 and 5.

The tensile strength at break for films produced by the blown film process shows higher value in MD than in TD. This observation was usually governed by amorphous phase orientation and amorphous phase orientation along MD was probably higher than that along TD. Figure 4.23 reveals that at fixed BUR, tensile strength in MD increased when DR increased. At fixed DR, tensile strength in TD increased when BUR increased. At BUR 3 and DR 1-5 the tensile strengths at break in MD were significantly higher than those in TD, due to more molecular orientation in MD. At BUR 5 and DR 1-5 the tensile strengths at break in MD and TD were not different which shows a more balanced molecular orientation in both directions (Figure 4.24). The transformation of the parent crystalline lamella structure into fibrils on drawing results in an increase of orientation for both the crystalline and amorphous phases. Consequently, the molecules in this latter phase become taut tie and are close packed leading to the increase of tensile strength with draw ratio (Park *et al.*, 1996).

Figures 4.25-4.26 show the tensile strength at break of the LLDPE/NR blends at composition 90/10 wt% as function of draw ratio. The strength of sample increased when draw ratio increased due to higher molecular orientation. Tensile strength for the composition 80/20 wt% are shown in Figures 4.27-4.28.

4.6.1.2 Tensile Strength at Break for LLDPE and LLDPE/NR Blends Produced from Chill Roll Cast Film Process.

Tensile strength at break for chill roll cast film of pure LLDPE is shown in Figure 4.29. Tensile strength in MD at DR 1 exhibited value around 9 MPa in MD and then increased abruptly to 28 MPa at DR 5.5. But tensile

strength in TD slightly increased from 4 to 11 MPa at DR 1 to 5.5 respectively. This was due to the effect of molecular orientation. In the chill roll cast film process uniaxial molecular orientation was dominant during drawing, causing an imbalance in molecular orientation between MD and TD. At high DR molecule tended to orient in MD only. A significant higher tensile strength was observed. Tensile strengths at break for LLDPE/NR blends at compositions 90/10, 80/20 and 70/30 wt% are shown in Figures 4.30-4.32.

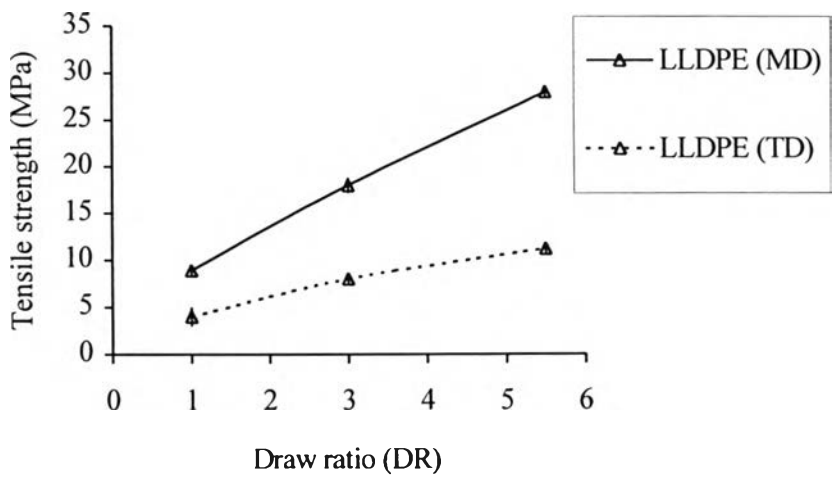

Figure 4.29 Tensile strength at break for LLDPE cast films at DR 1, 3 and 5.5.

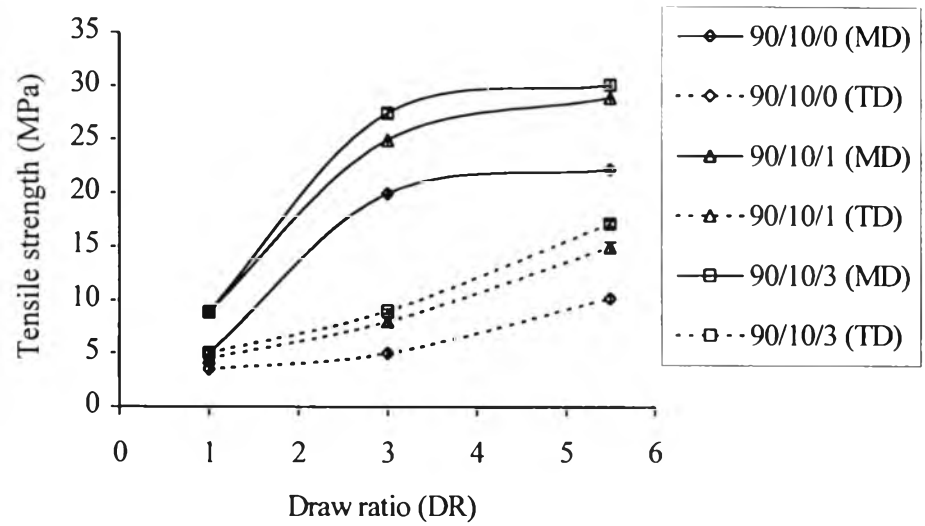

Figure 4.30 Tensile strength at break for LLDPE/NR cast films at composition 90/10 wt% in MD and TD at DR 1, 3 and 5.5.

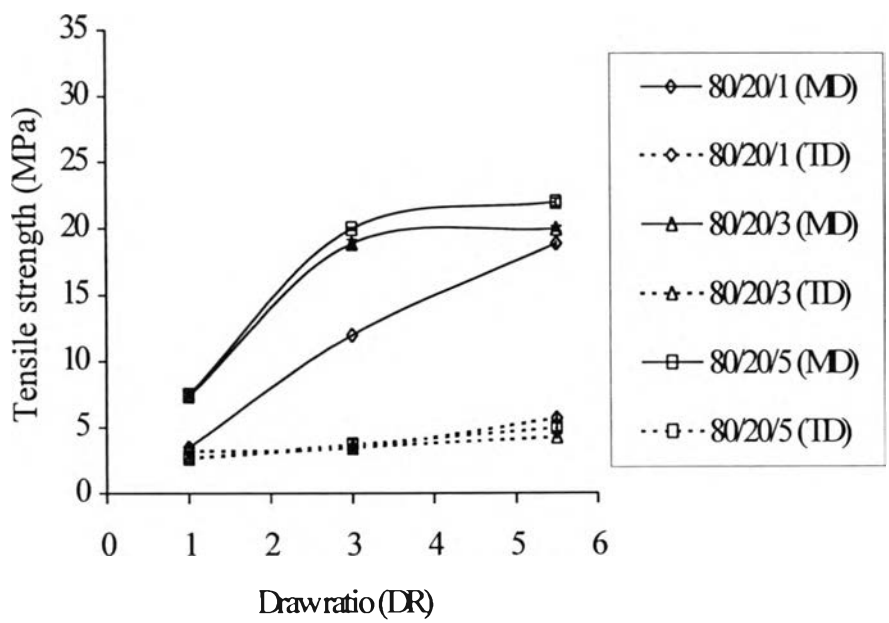

Figure 4.31 Tensile strength at break for LLDPE/NR cast films at composition 80/20 wt% in MD and TD at DR 1, 3 and 5.5.

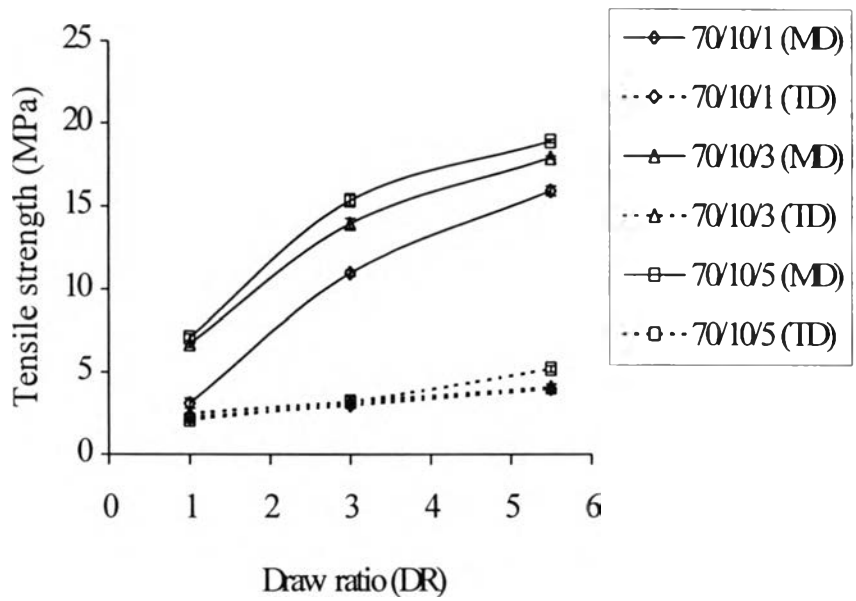

Figure 4.32 Tensile strength at break for LLDPE/NR cast films at composition 70/30 wt% in MD and TD at DR 1, 3 and 5.5.

4.6.1.3 Effect of MA and NR Content on Tensile Strength of LLDPE and LLDPE/NR Blend Films Produced from Blown Film and Chill Roll Cast Film Process.

Besides the drawing process conditions, the strength of LLDPE/NR blends films are also dependent on MA compatibilizer.

Addition of NR 10 wt% without MA showed a negative effect on the tensile strength at break for films from the blown film process. This was due to the lack of interfacial adhesion between LLDPE and NR phases. The poor adhesion between the NR dispersed phase and the LLDPE matrix resulted in higher actual stresses in the LLDPE matrix for a given applied load and caused a rapid failure of the film. On the contrary (at fixed BUR 3 and DR 5), addition of MA 1-3 wt% caused a significant increase of tensile strength in both MD and TD for films from the blown film process. For example (see Figure 4.25), tensile strength for LLDPE/NR blends at composition 90/10 wt% without MA exhibited value around 4 MPa and 5 MPa in MD and TD respectively. After addition of MA 1 wt% an increase of tensile strength to about 12 MPa in both MD and TD at DR 5 was observed. Further addition of MA (to 3 wt%) caused an increase in the tensile strength of blend films to 13 and 12 MPa in MD and TD at DR 5. It can be concluded that MA can improve the interfacial adhesion and thus increase the tensile strength of blend films. Tensile strength values at composition 80/20 wt% for blown film process are shown in Figures 4.27-4.28

Figures 4.29 shows tensile strengths of pure LLDPE and LLDPE/NR cast films processed at DR 1-5.5. Tensile strength for chill roll cast films also showed similar results. For the composition 90/10 wt% without MA the tensile strength had the lowest value around 22 and 10 MPa in MD and TD at DR 5.5. By adding 1-3 wt% MA, the tensile strength increased up to 30 in MD

and 17 in TD at DR 5.5. With high amount of NR, tensile strength decreased but the effect of DR on tensile strength was more pronounced in MD than in TD. It was also found that the tensile strength of compositions 80/20 and 70/30 wt% LLDPE/NR blends increased with MA amount as shown in Figures 4.31-4.32.

4.6.1.4 Effect of Biaxial and Uniaxial Orientation in Blown film and Chill Roll Processes on Tensile Strength at Break of LLDPE Films

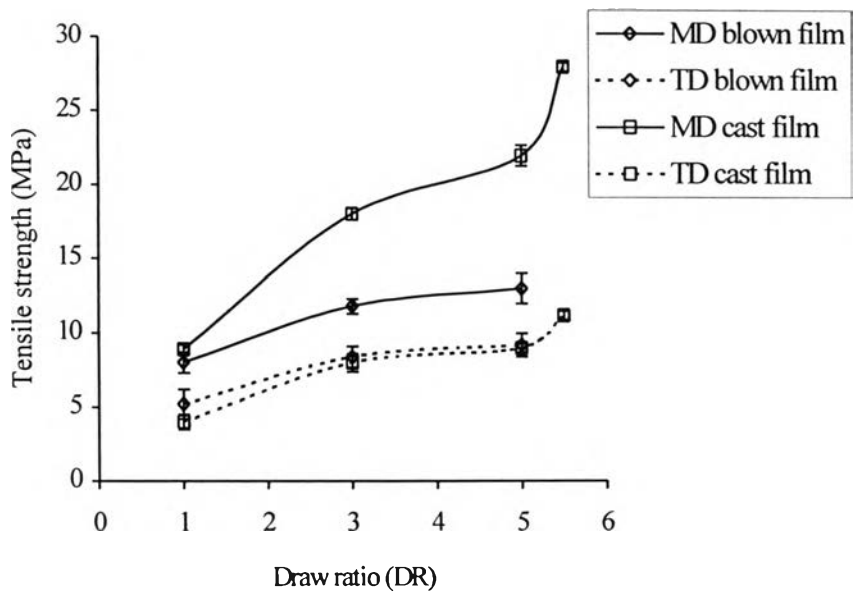

Figure 4.33 Tensile strength at break for LLDPE blown films at BUR 3 and films from chill roll cast film process.

The tensile strength of chill roll films is much higher than that of the blown films especially in MD. This is due to the difference in molecular orientation between film from blown film and chill roll cast film processes. Figure 4.33 shows the tensile strength at break of film from blown film about 8

and 5 MPa in MD and TD at DR 1 and the tensile strength reached to 13 and 9 MPa in MD and TD at DR 5. Tensile strength of film from chill roll cast film about 9 and 4 in MD and TD at DR 1 and then increased abruptly to 28 MPa in MD and 11 MPa in TD at DR 5.5. The superior properties, especially in MD, of chill roll cast films are due to faster cooling.

4.6.2 Impact Strength

In high-speed puncture impact testing method, the energy required to break the specimens is determined from the highest force causing puncture impact to the film or sheets. Therefore, the ability of material to resist sudden load can be influenced by many factors as following.

4.6.2.1 Effect of Process Variables BUR and DR in Blown film Process on Impact Strength of LLDPE and LLDPE/NR Blend Films

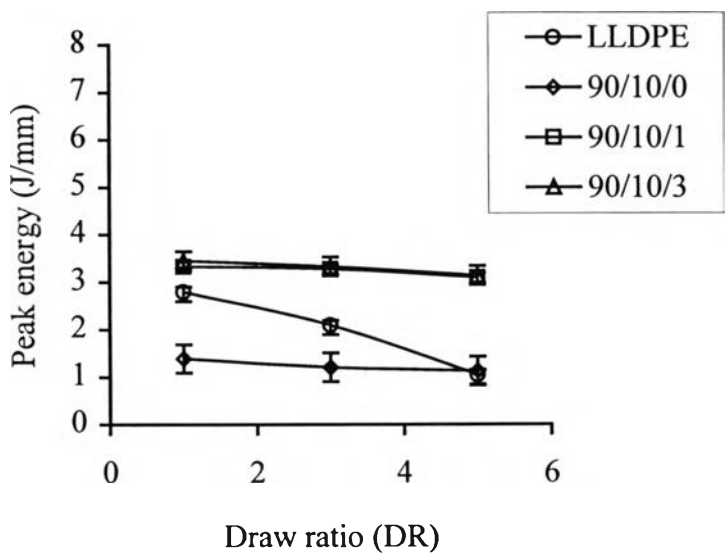

Figure 4.34 Impact strength of LLDPE and LLDPE/NR blown films at composition 90/10 wt% at BUR 3.

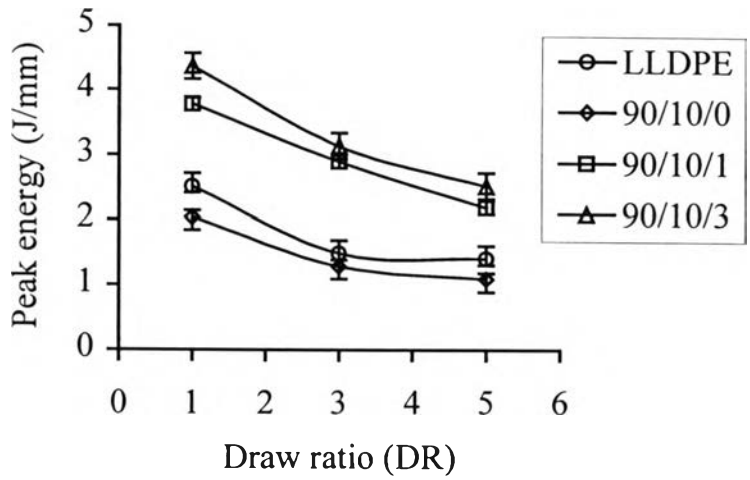

Figure 4.35 Impact strength of LLDPE and LLDPE/NR blown films at composition 90/10 wt% at BUR 5.

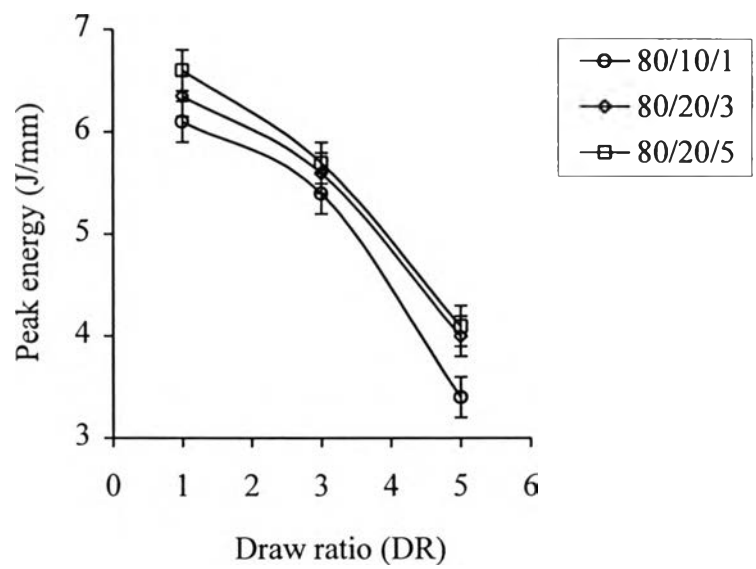

Figure 4.36 Impact strength of LLDPE/NR blown films at composition 80/20 wt% at BUR 3.

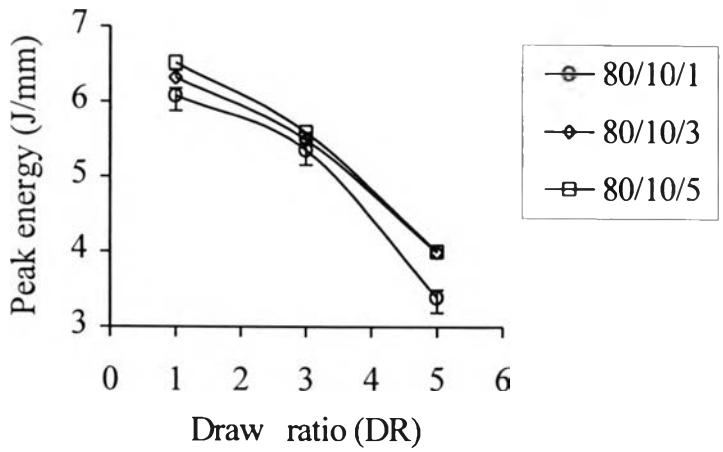

Figure 4.37 Impact strength of LLDPE/NR blown films at composition 80/20 wt% at BUR 5.

In case of blown film, the effect of molecular orientation on impact strength could be seen from Figures 4.34-4.37. Impact strength decreased when DR increased. On the contrary, impact strength increased when BUR increased. When a sudden load was applied, the failure of film propagated in the direction of chain alignment. For LLDPE at BUR 3 and DR 5 the molecules were oriented mainly in machine direction, impact strength exhibited values around 1 J/mm (Figure 4.34). At BUR 5 impact strength was increased to 1.5 J/mm as shown in Figure 4.35. It showed that, at DR 5 and BUR 5 when less difference of molecular orientation in machine and transverse direction was formed, molecules formed a network and tended to have better resistance to the deformation of film. In other word, high BUR led to more balanced orientation as well as higher degree of planar orientation in both MD and TD. Impact strength data for composition 80/20 are shown in Figures 4.36-4.37.

4.6.2.2 Impact Strength of LLDPE and LLDPE/NR Blend Films Produced from Chill Roll Cast Film Process.

The uniaxial orientation in chill roll cast film caused a rapid deformation of films. It was found that molecular orientation in MD was higher than TD especially at high DR. This inferred that more imbalance molecular orientation provided less ability to resist impact load. In other word, for uniaxial orientation only molecules aligned in MD could bear the impact force but in other direction only fragment of molecules carried the load and thus these two other directions became weak. From Figures 4.38-4.40 show that impact strength decreased when DR increased.

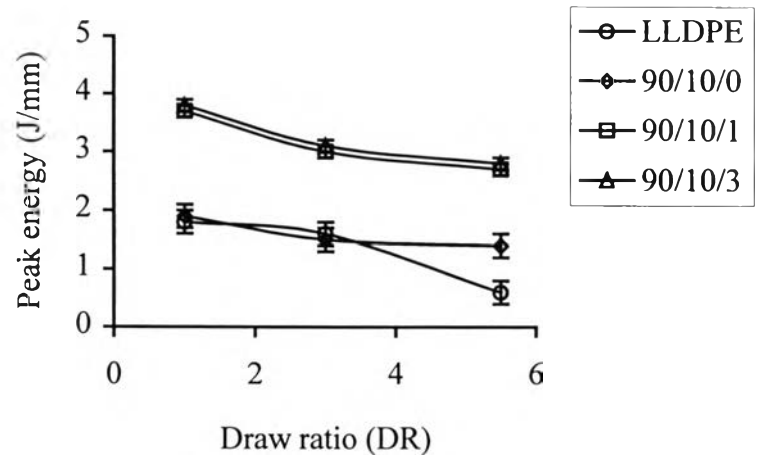

Figure 4.38 Impact strength of LLDPE and LLDPE/NR cast films at composition 90/10 wt%.

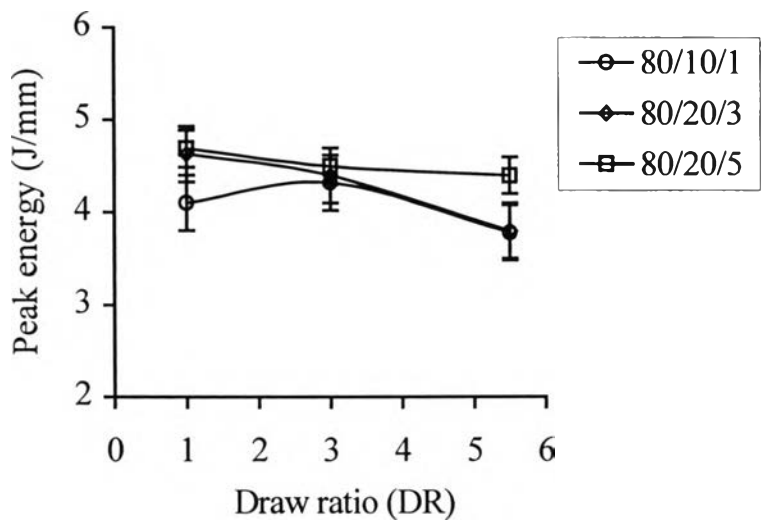

Figure 4.39 Impact strength of LLDPE/NR cast films at composition 80/20 wt%.

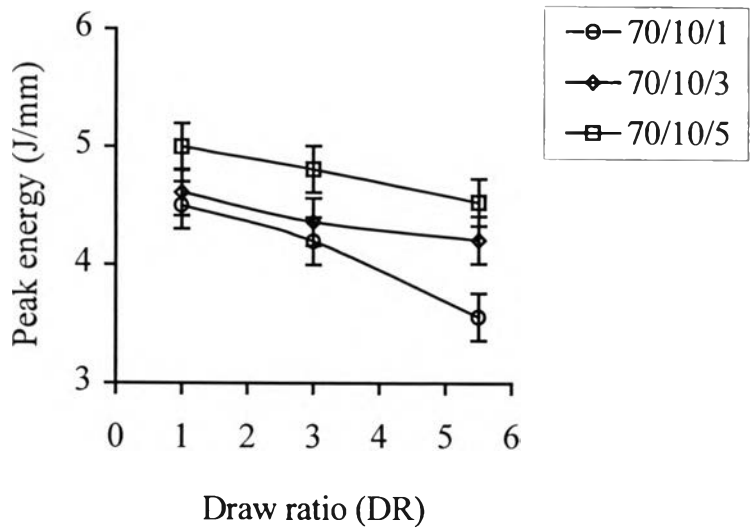

Figure 4.40 Impact strength of LLDPE/NR cast films for composition 70/30 wt%.

4.6.2.3 Effect of MA and NR Content on Impact Strength of LLDPE and LLDPE/NR Blend Films from Blown Film and Chill Roll Cast film Processes

Addition of 10 wt% NR without MA caused a reduction of impact strength of films from blown film process (Figure 4.34). This inferred that NR was not capable to absorb energy as expected due to poor adhesion between the two phases. Moreover, LLDPE/NR blends at composition 90/10 wt% with 1 wt% MA showed much improved impact strength. This was due to the amorphous nature of NR able to absorb a lot of energy and the good adhesion to allow the transfer of impact load between two phases. Increased amounts of NR and MA induced higher impact strength. Impact strength results for composition 80/20 wt% are shown in Figures 4.36-4.37.

In the case of chill roll cast films, addition of 10 wt% NR without MA exhibited the lowest impact strength while adding 1 wt% MA increased impact strength to about twice as shown in Figure 4.38. Impact strength results for films produced from chill roll cast film process for compositions 80/20, 70/30 wt% are shown in Figures 4.39-4.40.

4.6.2.4 Effect of Biaxial and Uniaxial Orientation in Blown Film and Chill Roll Cast Film Processes of LLDPE and LLDPE/NR Blend Films

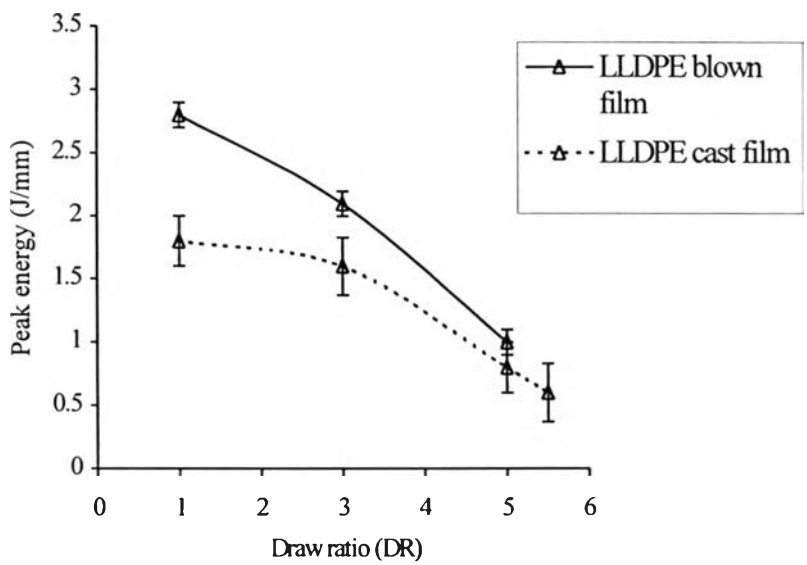

Figure 4.41 Impact strength of LLDPE films produced by blown film at BUR 3 and chill roll cast film processes.

The impact strengths of cast films were lower than that of blown films because of high molecular orientation in MD direction (Figure 4.41). It was seen clearly that impact strength of blown film at BUR 3 decreased when DR increased from 3 to 5. This was due to the orientation of molecules tended to align in machine direction and led to different orientations between MD and TD.

The uniaxial orientation caused a rapid deformation of films. Orientation of molecules generally increased impact strength if the impacting force was parallel to the orientation and the impact strength was poorer if the force was applied perpendicular to the orientation. In practical situations, the impact loads might come from any directions, film or sheet always broke in the weakest direction (Capiati *et al.*, 1996).

4.6.3 Tear Resistance

Tear resistance has been widely considered for plastic films and thin sheets used in packaging applications. The Elmendorf test method provides a controlled means for tearing specimens at strain rates approximating some of those find in actual packaging service.

Due to orientation during their manufacture, plastic films and sheeting frequently show markedly anisotropy in their tear resistance. This is further complicated by the fact that some films elongate greatly during tearing, even at the relatively rapid rate of loading encountered in this test. The degree of this elongation is dependent on film orientation and the inherent mechanical properties of the polymer from which it is made.

4.6.3.1 Effect of Process Variables BUR and DR on Tear Resistance of LLDPE and LLDPE/NR Blend Films Produced from Blown Film Process.

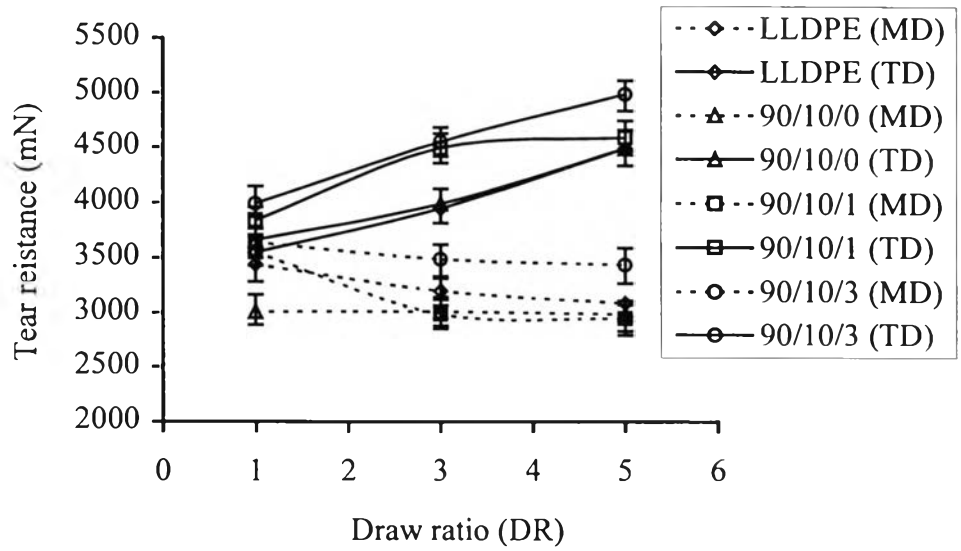

Figure 4.42 Tear resistance of LLLDPE and LLDPE/NR blown films at composition 90/10 wt% at BUR 3.

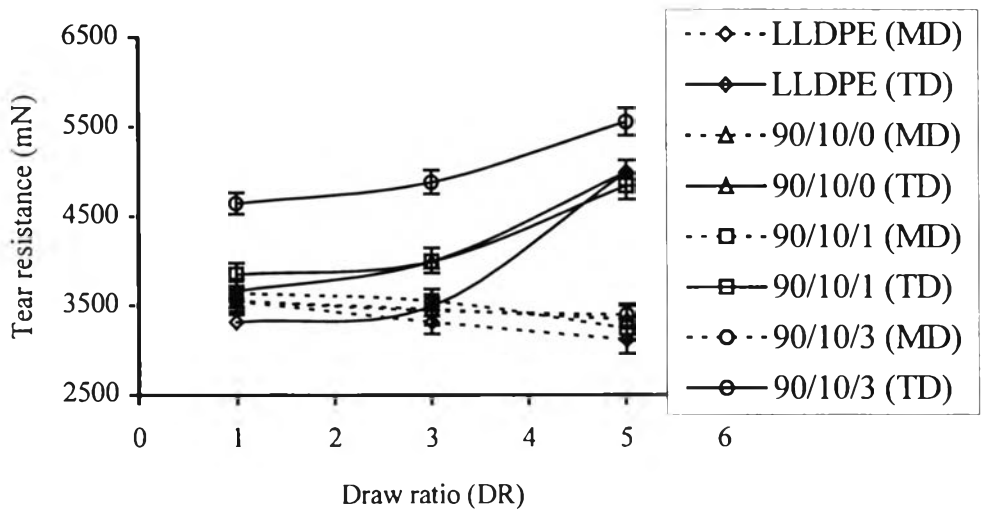

Figure 4.43 Tear resistance of LLLDPE and LLDPE/NR blown films at composition 90/10 wt% at BUR 5.

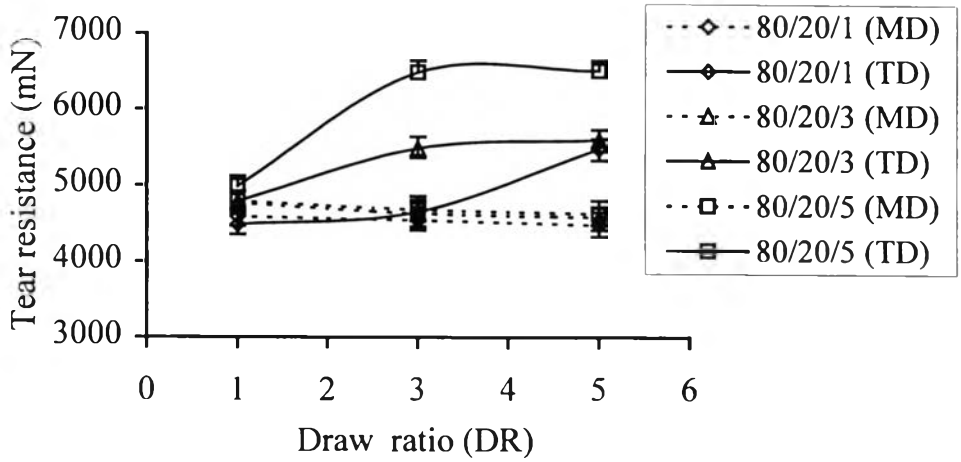

Figure 4.44 Tear resistance of LLDPE/NR blown films at composition 80/20 wt% at BUR 3.

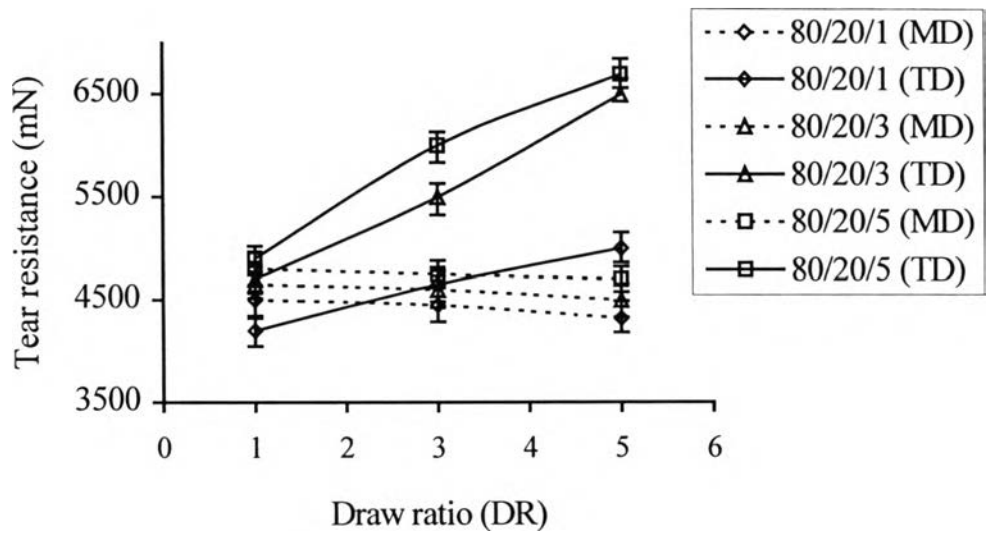

Figure 4.45 Tear resistance of LLDPE/NR blown films at composition 80/20 wt% at BUR 5.

The main important effects for tear resistance are orientation of molecules, size and distribution of lamellae stack that are perpendicular to the force direction (Brydson, *et al.*, 1995). In blown film process, increasing DR to 3 and 5 induced molecule or chain of polymer to highly orient in MD. So, higher tear resistance in TD was observed. It was found that at fixed BUR, tear resistance was sharply increased to almost 4,500 mN in TD at DR 5 for LLDPE (Figure 4.42); i. e. tear resistance increased with DR. Nevertheless, tear resistance in MD slightly dropped with increasing BUR. Tear resistance in TD was always higher than in MD. Less energy was needed to break weak intermolecular force between polymer chains that oriented in machine direction. But more energy was required to tear polymer chains that aligned perpendicularly to the direction of force (TD). Tear resistance for LLDPE/NR blends at compositions 90/10 and 80/20 wt% are shown in Figures 4.42-4.45.

4.6.3.2 Tear Resistance of LLDPE and LLDPE/NR Blend Films Produced from Chill Roll Cast Film Process.

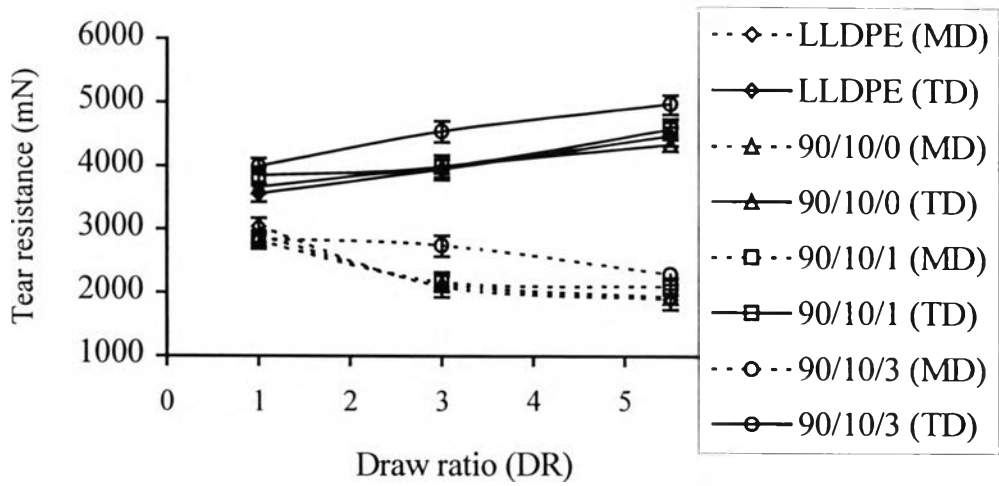

Figure 4.46 Tear resistance for LLDPE and LLDPE/NR cast films at composition 90/10 wt%.

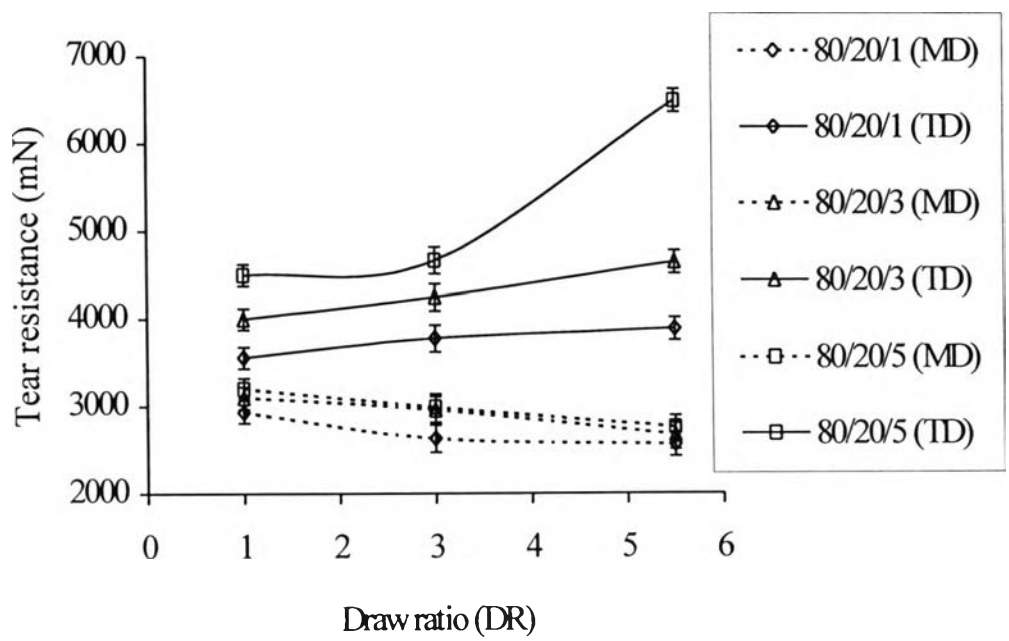

Figure 4.47 Tear resistance for LLDPE/NR cast films at composition 80/20 wt%.

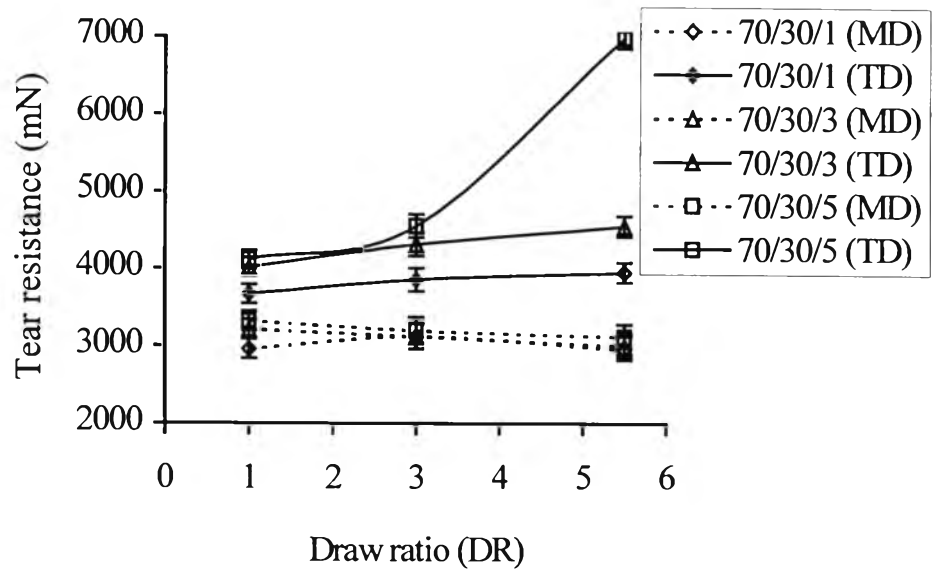

Figure 4.48 Tear resistance for LLDPE/NR cast films at composition 70/30 wt%.

From Figures 4.46-4.48 show tear resistance of film produced from chill roll cast film process. It was found that tear resistance in MD decreased when increasing DR. But tear resistance in TD increased when increasing DR. This was due to the effect of molecular orientation. For example, tear resistance of LLDPE exhibited value around 3,000 and 3,500 mN in MD and TD at DR 1. Increasing DR to 5.5, tear resistance in TD increased abruptly to 4,500 mN while tear resistance in MD significantly decreased to 2,000 mN. Addition of NR and MA into LLDPE had significant improve tear resistance of LLDPE (see in 4.6.3.3).

4.6.3.3 Effect of NR and MA Content on Tear Resistance of LLDPE and LLDPE/NR Blend Films from Blown Film and Chill Roll Cast Film Processes

Tear resistance for blown films at composition 90/10 wt% are shown in Figures 4.42-4.43. Addition of 10 wt% NR at BUR 3 did not alter tear resistance of LLDPE, but at BUR 5 tear resistance increased. Tear resistance in TD increased further with addition of MA for 90/10 LLDPE/NR blends. But tear resistance in MD slightly dropped as NR content increased; tear resistance in TD also increased. From figure 4.42 pure LLDPE had value around 4500 mN at BUR 3 and DR 5; tear resistance of blends at composition 90/10 with 3 wt% MA exhibited value nearly 5,000 mN. Figures 4.44 and 4.45 show the tear resistance of LLDPE/NR blends at composition 80/20 wt%. It could be seen that tear resistance of the blends in both MD and TD were significant higher than pure LLDPE. Moreover, MA can improve tear resistance of the blends. It was found that tear resistance increased when MA loading increased due to an increase in interfacial adhesion.

Tear resistance for chill roll cast films showed that tear resistance in TD increased when NR loading increased as shown in Figure 4.46 for composition 90/10 wt%. But tear resistance in MD decreased. This was due to the chill roll process, which allowed molecules to orient especially in MD. So, at higher draw ratios a significant decrease of tear was observed. Figures 4.47 and 4.48 show a very interesting point: 20 and 30 wt% NR loading caused a significant increase of tear in TD, reaching values around 6,000 and 7,000 at DR 5.5 respectively. Although, tear resistance in MD should be decreased as draw ratio increases in the chill roll process, adding NR 20 and 30 wt% together with 1-5 % MA could improve tear resistance of film in MD. The NR phase absorbs energy and prevents tearing of film.

4.6.3.4 Effect of Biaxial and Uniaxial Orientation in Blown Film and Chill Roll Cast Film Processes on Tear Resistance of LLDPE and LLDPE/NR Blend Films

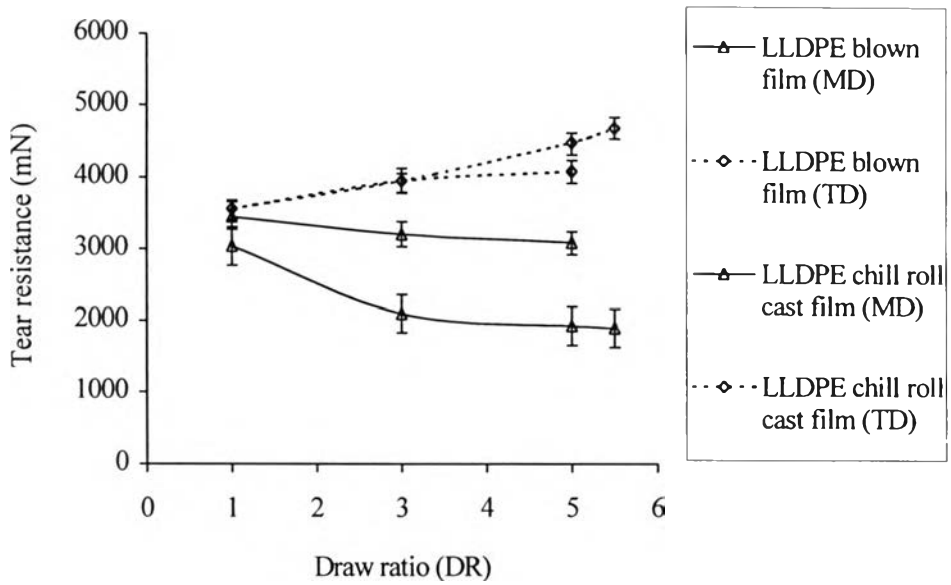

Figure 4.49 Tear resistance of film from blown films at BUR 3 and chill roll cast film processes.

The tear resistance of LLDPE films from chill roll cast film process was higher than film from blown film process, especially in TD direction. On the other hand, the tear resistance of films from chill roll casting process was slightly lower than that of films from blown film process in the MD direction. This can be explained in terms of the orientation of molecules already discussed in previous sections (Figure 4.49).